Colloquium: Heat flow and thermoelectricity in atomic and molecular junctions

Yonatan Dubi* and Massimiliano Di Ventra†

Department of Physics, University of California–San Diego, La Jolla, California 92093, USA

(Received 2 October 2009; published 29 March 2011)

Advances in the fabrication and characterization of nanoscale systems now allow for a better understanding of one of the most basic issues in science and technology: the flow of heat at the microscopic level. In this Colloquium recent advances are surveyed and an understanding of physical mechanisms of energy transport in nanostructures is presented, focusing mainly on molecular junctions and atomic wires. Basic issues are examined such as thermal conductivity, thermoelectricity, local temperature and heating, and the relation between heat current density and temperature gradient—known as Fourier's law. Both theoretical and experimental progress are critically reported in each of these issues and future research opportunities in the field are discussed.

DOI: 10.1103/RevModPhys.83.131 PACS numbers: 65.80.−g, 68.65.−k, 74.25.fg, 79.10.−n

CONTENTS

I. Introduction 131
II. Heat Current and Thermal Conductivity 133
A. Definitions 133
B. Experiment 134
C. Theoretical methods 135
1. Single-particle scattering approach 135
2. The role of interactions 137
3. Molecular dynamics 138
III. Local Temperature and Heating 139
A. General remarks 139
B. Heating in current-carrying nanostructures: Theory 140
1. Various definitions of out-of-equilibrium temperature 140
2. Ionic heating 141
3. Electron heating 142
4. Ionic cooling 142
C. Heating in current-carrying nanostructures: Experiment 142
D. Fourier's law at the nanoscale 144
IV. Thermopower 145
A. Introduction and basic definitions 145
B. Experiments on thermopower at the nanoscale 145
C. Theoretical methods 147
1. Single-particle theory of thermopower 147
2. An open quantum system approach 149
V. Summary and Future Prospects 151
A. Future prospects 151
B. Final thoughts 151

I. INTRODUCTION

Understanding how heat is carried, distributed, stored, and converted in various systems has occupied the minds of many scholars for centuries. Recently, the problem has garnered even more attention and has grown considerably in importance. This is not due only to purely academic reasons: Its practical impact on society has been recognized as one of the most critical programs for the development of the necessary resources to sustain the future welfare of mankind (USDOE, 2009).

In conjunction with these motivations, research seems to suggest that nanoscale systems (such as carbon-based nanostructures, organic molecules, etc.) may be good candidates for such technological advances. For instance, the flow of heat in nanoscale systems may be harnessed via thermoelectric effects (Majumdar, 2004; Bell, 2008; Rodgers, 2008) to generate heat-voltage converters, which (if their efficiency can be improved) may have real impact on global energy consumption. Other interesting applications, such as nanoscale local refrigerators (Shakouri, 2006), thermal transistors (Giazotto *et al.*, 2006; Li *et al.*, 2006; Franceschi and Mingo, 2007; Lo *et al.*, 2008; Saira *et al.*, 2007), thermal rectifiers (Terraneo *et al.*, 2002; Li *et al.*, 2004a, 2004b; Segal and Nitzan, 2005; Wu and Li, 2007; Yang *et al.*, 2009), nanoscale radiation detectors (Giazotto *et al.*, 2006), and even thermal memory and logic gates (Wang and Li, 2007, 2008) add to the importance and interest of this research field.

In spite of the recent advances, this research program still presents quite a few challenges related to the intrinsic nonequilibrium nature of the problem. In the presence of a heat current, quite generally, both electrons and ions may be very far from their equilibrium state. In addition, they are in interaction with each other and, at the same time, in *dynamical* interaction with one or more environments.

To complicate matters, heat flow is in many ways (as we will discuss in detail in the following sections) fundamentally different from charge flow. Therefore, many of the theoretical tools which are used to describe charge transport cannot be straightforwardly and uncritically extended to the study of heat transport. From an experimental perspective,

*Current address: School of Physics and Astronomy, Tel-Aviv University, Tel Aviv 69978, Israel.
dubij76@gmail.com
†diventra@physics.ucsd.edu

studying energy flow at the nanoscale is in several ways more challenging than studying charge transport, one reason being that no simple device analogous to an ''ammeter'' is on hand to measure energy currents. Furthermore, the scale of achievable thermal conductivities is generally much smaller than that of electrical conductivities (Majumdar, 2004). Consequently, one has to necessarily introduce models by which the thermal conductance can be *deduced* from measurable quantities such as charge current, voltage, and temperature. In addition, measurement schemes with macroscopic probes are necessarily used so that the channeling of heat across only the junction is difficult to achieve.

In this Colloquium we will discuss all these issues at the microscopic level. The basic systems we will consider consist of a nanoscale junction, namely, two leads connected by a nanoscale element, with possibly a third lead controlling some state variable of the system, e.g., its local temperature. Typical examples are point contacts or quantum dots placed between a two-dimensional electron gas (van Houten *et al.*, 1992a; Staring *et al.*, 1993; Molenkamp *et al.*, 1994; Godijn *et al.*, 1999; Scheibner *et al.*, 2007), a molecule trapped between a substrate and a scanning tunneling microscope (STM) tip (Reddy *et al.*, 2007; Baheti *et al.*, 2008), metallic wires (Ludoph and Ruitenbeek, 1999), carbon nanotubes (Kim *et al.*, 2001; Yu *et al.*, 2005), or silicon nanowires (Boukai *et al.*, 2007; Hochbaum *et al.*, 2007) between two metal contacts, etc. Figure 1 shows a schematic representation of the different systems we consider. The leads are held at different temperatures, which allow for the flow of energy (and possibly charge) through the junction. Here, we point out that, due to space limitations, we will not be able to discuss the entire class of systems collectively known as ''nanomaterials''—composite layers of various materials fabricated on nanometer scales, which show unique electronic properties, often engineered by adding scattering mechanisms (for instance, boundary scattering) that may be beneficial for energy applications (Majumdar, 2004; Volz, 2009). The interested reader may refer to Chen (2005) for systems other than those presented here.

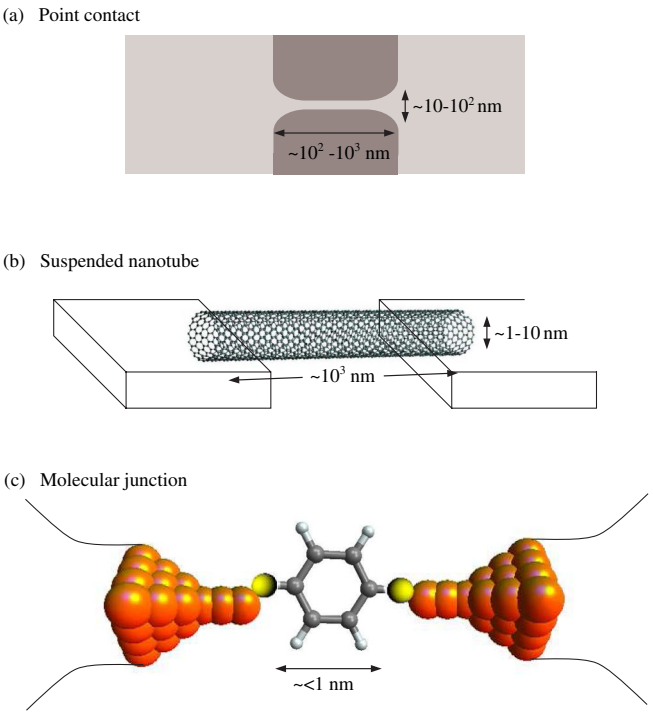

FIG. 1 (color online). Schematic representation of the different systems we consider in this Colloquium, ranging from metallic point contacts to molecular junctions.

To make the Colloquium easier to follow, we have divided it into three main (yet closely related) subtopics. The first one is the transport of heat through the system by phonons (lattice vibrations) and electrons, which (in linear response) is mainly characterized by the thermal conductivity κ. This issue has already been reviewed elsewhere (Galperin *et al.*, 2007a; Wang, *et al.*, 2008), emphasizing the effects of vibrations and focusing primarily on the method of nonequilibrium Green's functions. To make the present Colloquium complete, and in order to highlight the various theoretical methods and the open questions that still pertain to this subject, we give it some space here too. In particular, we will discuss the different processes that contribute to κ and their importance in nanoscale junctions.

The second subject is that of the local temperature and heating inside the nanoscale system. This issue is particularly subtle, precisely because we are dealing with a nonequilibrium process where a temperature difference is set at the two sides of the nanojunction. We will address several experimental and theoretical issues and fundamental open questions, such as how does one define a local temperature at the nanoscale in a nonequilibrium situation? What determines the local temperature and the temperature profile along the system?

As a corollary to the above studies we are finally led to analyze a nearly two-century old and important physical law, which so far has eluded a satisfactory theoretical understanding, namely, Fourier's law (FL). This law, as originally formulated, states that in the presence of a temperature difference between the two leads (i) a temperature gradient develops, (ii) the energy current density is proportional to it, and (iii) the constant of proportionality is independent of system size. While FL was empirically postulated for bulk systems almost two centuries ago (Fourier, 1822) and has been derived phenomenologically for phonons more than 80 years ago (Peierls, 1929), no simple proof of its validity (or invalidity) has ever been derived from first principles, nor do we have a well-defined set of conditions to determine its validity for a given system (Bonetto *et al.*, 2000). As we will emphasize later, the issue has everything to do with the difficulty in defining the basic quantities that enter its formulation—namely, the local temperature and heat current—from a microscopic, quantum mechanical point of view.

The final issue is that of the interrelation between the heat flow and the electron transport through the junction, which can be collected under the general name of ''thermoelectricity.'' The central quantity here is the thermopower (or Seebeck coefficient) S, which describes the voltage drop generated by a temperature difference. A sample of important open questions for this topic are what are the different mechanisms contributing to thermoelectricity? Are they properly taken into account in the present theories? What are the state-of-the-art experiments, and are their results interpreted satisfactorily?

All of these issues and open questions will accompany us for the full length of this Colloquium. We will stress their importance for both their fundamental character as well as their impact in possible technological applications. We will finally point out possible future research directions that could explore them in more depth.

The Colloquium is organized as follows. In Sec. II we discuss heat flow in nanoscale systems due to phonons, electrons, and their mutual interaction, and describe the different processes which contribute to it. We review both theoretical tools and state-of-the-art experiments for measuring heat flow in nanostructures. We devote Sec. III to local temperature effects and proceed to discussing Fourier's law. In Sec. IV we discuss thermoelectric effects in nanoscale junctions. We give a detailed account of present theoretical tools and discuss recent experiments, with emphasis on open issues in the field. Finally, we conclude in Sec. V with some prospects for the future of the field.

II. HEAT CURRENT AND THERMAL CONDUCTIVITY

We start by reviewing the topic of heat current and thermal conductivity of nanoscale junctions. We will not present full derivations of the methods and results. Rather, we will outline only the main theoretical tools. The interested reader may find extensive accounts in recent reviews (Galperin *et al.*, 2007b; Dhar, 2008; Wang *et al.*, 2008) or books (Akkermans and Montambaux, 2007; Di Ventra, 2008), where these methods are discussed in detail. In addition, we will review recent experimental advances in measurements of the thermal conductivity in nanoscale systems, with an emphasis on the measurement process itself and open questions.

A. Definitions

When a nanoscale junction is placed in contact with leads held at different temperatures, energy flows through it. The original qualitative description for this phenomenon in bulk materials is attributed to Fourier (1822), and amounts to Fourier's law which states that a temperature gradient ∇T induces a thermal current density linearly proportional to it, namely,

$$j_{th} = -\kappa \nabla T, \tag{1}$$

where j_{th} is the heat current density (which may contain both phonon and electron contributions, see below), and κ is the thermal conductivity (such an equation is usually valid only in the linear regime).

In Secs. III.B and III.D we will expand more on the significance of the term "temperature" for a system out of equilibrium and its different definitions. Here we anticipate that whenever we do not discuss its meaning explicitly we call temperature that which is measured by a local thermal probe weakly coupled to the system and whose temperature has been adjusted so that the system dynamics is minimally perturbed (Di Ventra, 2008). This defines what we will later call a *temperature floating probe* (Dubi and Di Ventra, 2009c, 2009d). Note that we do not define it in terms of a probe adjusted so that the thermal current between the system and probe is zero, precisely because we do not have means to directly measure the thermal current (although these two definitions may give the same quantitative results). In addition, one needs to keep in mind that while this is an operational definition of temperature out of equilibrium, its actual experimental determination is far from trivial at the present.

The validity of Eq. (1) in nanoscale junctions is discussed in detail in Sec. III.D. Here we are mainly interested in the theoretical understanding and measurement of j_{th} and κ, assuming that Fourier's law is indeed valid. A relation between the formalism described below [Landauer's formula (6)] and Fourier's law can be determined, which requires calculation of thermal conductances at larger and larger length scales. Such derivation, discussed elsewhere (Dhar, 2008), implies going beyond the realm of nanoscale junctions and will thus not be discussed in detail here.

It is also convenient to introduce the thermal conductance, which is the ratio between the total heat current J_{th} and temperature difference $\Delta T = T_R - T_L$,

$$\sigma_{th} = -\lim_{\Delta T \to 0} \frac{J_{th}}{\Delta T}. \tag{2}$$

If the sample is uniform with a constant cross section A and length L, the thermal conductance is related to thermal conductivity κ via $\sigma_{th} = (A/L)\kappa$. If the sample is not uniform, then the relation between thermal conductance and conductivity depends on the microscopic details of the system. In addition, in analogy with electric circuit theory, it is convenient to define the thermal resistance, being the reciprocal of the thermal conductance $\rho_{th} = \sigma_{th}^{-1}$.

Energy can be carried through a nanoscale junction (or through a solid) either by lattice vibrations (phonons) or by electrons, or both.[1] In insulating bulk materials the electronic contribution is negligible, while it is sizable in bulk metals. This simple distinction is less obvious in nanoscale junctions, where, due to the large current densities they can carry,[2] the two contributions may be equally important and need to be discussed on equal footing. For bulk insulating materials, the theory of phonon thermal conductivity based on the Boltzmann equation was derived by Peierls (1955)) [see also the detailed review by Carruthers (1961)]. The main idea is that κ is governed by phonon scattering, especially the so-called umklapp scattering (processes that do not conserve crystal momentum), whereby phonons scatter between states which are separated (in reciprocal space) by a reciprocal lattice vector.[3] Considering a phonon mean-free path l (mainly due to scattering by impurities), simple arguments

[1] At low temperatures, energy can also be carried by the electromagnetic environment (photons), an effect which was studied in mesoscopic systems (Schmidt *et al.*, 2004), but was not systematically addressed in nanoscale junctions.

[2] For instance, in an atomic quantum point contact of a nominal cross section of 0.1 nm^2 to a typical current of 1 μA corresponds a current density of about 10^9 A/cm^2. This is several orders of magnitude larger than in mesoscopic or bulk systems.

[3] For a homogeneous bulk system in which the umklapp processes are suppressed and only "normal" processes occur (namely, processes that conserve crystal momentum), energy can flow undisturbed, giving rise to a diverging κ, and such a system cannot reach local or global equilibrium.

lead to the following relation at high temperatures (in three dimensions) (Ashcroft and Mermin, 1976):

$$\kappa \approx \tfrac{1}{3} l v c_v, \tag{3}$$

where v is the velocity of sound and c_v is the phonon heat capacity at constant volume (in the above equation optical and acoustic phonons are considered on equal footing, although only the latter ones participate in heat transport). In a bulk metal a similar relation can be derived (Ashcroft and Mermin, 1976), where now l stands for the electronic mean-free path, c_v is the electronic heat capacity at constant volume, and v is the electron drift velocity. Here a comment is in order. In the case of electrons the heat (or thermal) current contains also a contribution from the variation of the number of particles. In fact, consider the thermodynamic relation (at constant volume) $\delta Q = d\mathcal{E} - \mu dn$, where Q and $\mathcal{E}$ are the heat and energy per unit volume, respectively, n is the particle number density, and μ the chemical potential. From this relation, dividing by the infinitesimal time interval dt, we obtain (e is the electron charge)

$$J_{th} = J_E - \frac{\mu}{e} J_e, \tag{4}$$

namely, for electrons the heat current has both a contribution from the energy current J_E and from the charge current J_e (there is no such term for phonons, since their number is not conserved). In this Colloquium, we will use the terms "energy current" and "heat (thermal) current" interchangeably, but with the understanding that, in the case of electrons, one must generally include a contribution from the variation of the number of particles [see also the discussion after Eq. (6)].

It is now natural to ask whether these arguments can be extended to the regime in which strong material inhomogeneities are the norm, as in nanoscale systems. Before we embark on this quest, however, it is worth asking why κ is such an important quantity in the first place, especially since measuring the thermal conductivity at the nanoscale is all but trivial. The answer is that κ contains information regarding two main processes relevant to the future applicability of nanoscale systems. The first is the rate at which energy is dissipated in and removed from the junction. This has an effect on the heating of the system, which may affect its structural stability. The second is that κ is an important (and limiting) factor in the efficiency of nanoscale systems as heat-voltage converters (as will be discussed more at length in Sec. IV). Therefore, according to the desired use, an ideal nanosystem should have opposite thermal properties: For current-carrying wires one wishes for a high thermal conductance that would allow heat to pass through the wire and prevent overheating, and for thermoelectric conversion one requires a thermal conductance as small as possible. These requirements make the understanding, predictability, and control of κ highly desirable.

B. Experiment

In this section we focus on the experimental measurements of the thermal conductivity in nanoscale systems. As already pointed out, a major difficulty in measuring κ (other than the usual ones related to any measurements at the nanoscale) stems from the simple fact that there is *no direct way* to measure a heat current. Indeed, the only directly measurable quantities are electrical currents, voltages, and temperatures (the latter are also typically measured via resistance measurements), and from these one deduces κ. The main limitation is that the value of κ as extracted from the experiment may then depend on the model used to describe the whole experimental setup or device, which may generate some ambiguity. Here we will describe some recent experiments, discuss the methods employed in deducing κ, and review some of the main results.

A conceptually simple way to measure the thermal conductance of a suspended nanojunction is the following. Consider the schematic system of Fig. 2. The heater coil is heated by passing a current through it. By measuring the current and the voltage through the heater coil, the power transferred through it is given by the well-known relation $P = IV$. This power increases the temperature of the coil to T_h. At the same time, the temperature of the sensor coil T_s is evaluated (by measuring its resistance, which is precalibrated to correspond to a given temperature). If the wire is suspended, then the entire heat current should be equal to the power supplied by the heater coil, $\dot{Q} = P$, which is related, in linear response, to the temperature difference by

$$\dot{Q} = -\sigma_{th}(T_h - T_s), \tag{5}$$

from which the thermal conductance σ_{th} can be evaluated, under the assumption that all the power supplied by the electric circuit flows through the junction without loss, and the thermal conductivity κ can then be extracted from a microscopic model that relates thermal conductivity to thermal conductance (see Sec. II.C). If, as indeed is the case in many experiments, some of the power is lost due to heat diffusion away from the contacts (e.g., into the substrate),

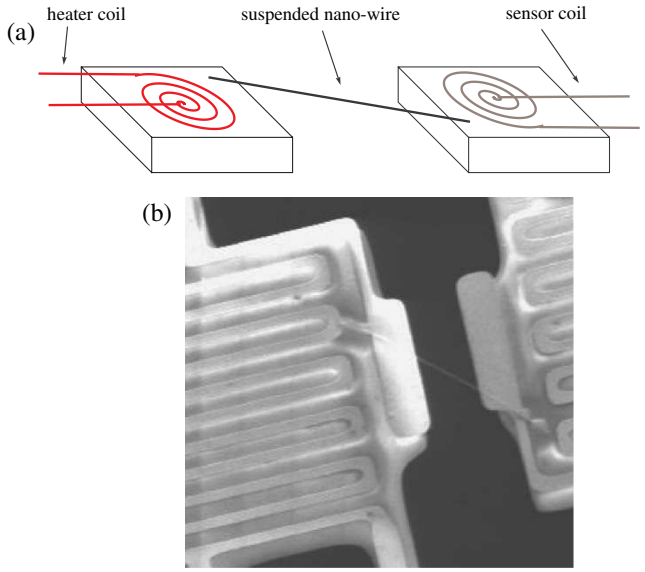

FIG. 2 (color online). (a) A schematic representation for a simple setup to measure the thermal conductance. (b) An actual device to measure the thermal conductance of boron nitrade nanotubes. From Chang *et al.*, 2006.

then the Joule heating is the sum of the heat flowing away through the contacts and that flowing through the wire.

This method seems very simple and was indeed employed to measure the quantum of thermal conductance (Schwab *et al.*, 2000). However, it needs to be acknowledged that it has obvious limitations. For one, dissipative effects at surfaces or local thermal gradients in the heating and cooling parts of the coils[4] may reduce the heat flow in the suspended wire. In addition, recent theoretical studies indicate that the contact thermal resistance between nanowires and substrate plays an important role in determining the overall thermal resistance (Zhong and Lukes, 2006; Chalopin *et al.*, 2008).

More difficult is the determination of the thermal conductivity κ from a model that includes all the effects of device geometry and dissipation through the contacts and substrates. Such models vary for different devices and geometries (Shi *et al.*, 2003; Chang *et al.*, 2006, 2008), but share the common feature that thermal conductances are treated on the same footing as classical (charge) conductances, with the same Kirchhoff-like laws for the addition of resistances in series ($\rho_{th} = \sum_i \rho_{th,i}$, with $\rho_{th,i}$ the thermal resistance of a single element of the circuit) and parallel ($\rho_{th}^{-1} = \sum_i \rho_{th,i}^{-1}$). Thus, the measured thermal conductivity may depend on the circuit model used, which makes it hard to compare between different experiments. This means that when performing a measurement, one is in fact measuring the thermal conductance of the system of interest embedded in that specific device. Nevertheless, this method was used to study the thermal conductivity of many nanoscale structures, mainly carbon nanotubes (Kim *et al.*, 2001; Shi *et al.*, 2003; Brown *et al.*, 2005; Chiu *et al.*, 2005; Fujii *et al.*, 2005; Yu *et al.*, 2005; Chang *et al.*, 2006, 2008), but also nanotubes of other materials (Li *et al.*, 2003; Chang *et al.*, 2008; Chen *et al.*, 2008). Some experimental features are universal, such as ballistic thermal conductance (Brown *et al.*, 2005; Chiu *et al.*, 2005), a value of κ which is orders of magnitude larger than the bulk value for carbon nanotubes (~ 3000 W/K at room temperature), an increase of thermal conductance with nanowire diameter, or a peak of the thermal conductance at $\sim$320 K (Kim *et al.*, 2001; Fujii *et al.*, 2005), attributed to the onset of umklapp phonon scattering processes. However, other features, such as the detailed power-law dependence of κ on temperature, vary between experiments, indicating that this is not a universal feature, and depend on the details of the experimental setup.

Other experimental approaches to measure κ have been introduced in the literature. For instance, Pop *et al.* (2006) used high currents to induce heating in a single-walled carbon nanotube, with a model to relate the current-voltage (I-V) characteristics to the high-temperature thermal conductance. In another example, the so-called 3ω method (Cahill, 1990; Lu *et al.*, 2001), was used to study nanotubes (Choi *et al.*, 2005, 2006; Bourgeois *et al.*, 2007). In this method, an ac current is applied to the sample which also acts as a heater. From a simple derivation one finds that the third harmonic of the voltage drop across the sample is related to the thermal conductivity of the sample (at small frequencies of the current). Using this method, they found a deviation of the thermal conductance from a cubic dependence on temperature for Si nanowires, indicating a dimensional crossover at low temperatures. Both these methods rely on current-induced self-heating of the sample (rather than direct heating by an external source). In a third example, laser-induced heating and Raman spectroscopy [already used in various nanoscale systems such as graphene ribbons (Calizo *et al.*, 2007; Balandin *et al.*, 2008)] were used to determine the local temperatures (Deshpande *et al.*, 2009; Hsu *et al.*, 2009) and extract the thermal conductance of carbon nanotube bundles. The main disadvantage of this method is that to obtain the thermal conductance one needs to assume a value for the optical absorbtion of the sample, which is usually unknown.

C. Theoretical methods

We now provide a brief description of the theoretical methods most commonly employed to describe energy flow, with an eye on their strengths and limitations.

1. Single-particle scattering approach

Many theoretical calculations of thermal conductance are based on an approach pioneered by Landauer (1957, 1970) in the context of charge transport in mesoscopic and nanoscopic systems (Datta, 1997; Imry, 1997; Di Ventra, 2008). The same ideas have been generalized to phonon transport through a nanoscale junction (Angelescu *et al.*, 1998; Rego and Kirczenow, 1998; Blencowe, 1999; Rego, 2001; Segal *et al.*, 2003; Blencowe, 2004; Dhar and Roy, 2006).

The basic tenet of this approach is that one assumes the leads are noninteracting [otherwise no closed form for the current can be obtained (Di Ventra, 2008)], so that a convenient basis, such as plane waves, can be chosen to develop state vectors for both types of particles, either phonons or electrons. As a further conceptual simplification, the leads are thought to be adiabatically ''connected'' to reservoirs whose only role is to define the occupation of the scattering states according to a local equilibrium Bose-Einstein (BE) distribution for phonons or a Fermi-Dirac (FD) distribution for electrons. Once this occupation is set, the particles are free to propagate in the leads before scattering at the lead-system interface. Charge and/or energy current is then determined by an electrochemical potential difference and/or a temperature difference between the reservoirs.

Most of the calculations also assume that the particles in the sample are either truly noninteracting or interacting at a mean-field level (which is the same from a formal point of view). In this case the current is simply proportional to the probability for the particles to cross the sample from one electrode to the other. For instance, in the case of phonon transport, phonon states at a given energy $\hbar\omega$ scatter off the junction and may be either transmitted through it or reflected back. The probability to be transmitted through the junction is characterized by the transmission coefficient $\mathcal{T}(\omega)$. The expression for the heat current is then simply

[4]Recall that one can destroy and create phonons at the surfaces of a material.

$$J_{th} = \int_0^\infty \frac{d\omega}{2\pi} \hbar\omega \mathcal{T}(\omega)(g_L - g_R), \tag{6}$$

where $g_{L(R)} = 1/[\exp(\hbar\omega/k_B T_{L(R)}) - 1]$ are the distribution functions of phonons in the left (right) lead. From J_{th} one can then evaluate the thermal conductance according to Eq. (2).

Within this approach the electronic contribution to the heat current is calculated similarly, where in Eq. (6) one makes two changes, namely, (i) the BE distribution functions are replaced by FD distributions, and (ii) the energy in each reservoir is measured from the respective electrochemical potential μ_L and μ_R for the left and right reservoirs, respectively, i.e., $\hbar\omega \to \hbar\omega - \mu_{L,R}$ [see Eq. (4)]. In a linear response this leads to the substitution $\hbar\omega \to \hbar\omega - (\mu_L + \mu_R)/2$ in the energy term that multiplies $\mathcal{T}(\omega)$ in Eq. (6).

To actually evaluate σ_{th}, one has to compute the transmission coefficient $\mathcal{T}(\omega)$. To this aim several methods have been employed, such as the use of continuum models (Angelescu *et al.*, 1998), the boundary condition method (Wang and Wang, 2006), the mode-matching method (Ando, 1991; Ting *et al.*, 1992; Khomyakov and Brocks, 2004), and scattering or transfer matrices (Tong *et al.*, 1999; Di Ventra and Lang, 2002). All of these methods are fundamentally equivalent, and, in fact, have their origin in the single-particle elastic scattering theory of conduction [see, e.g., Di Ventra (2008)], whereby one can write the transmission coefficient as a sum of all the partial probabilities of transmission $T_{if}(\omega)$ from one of the momentum states of the incoming (i) particle (whether electron or phonon) at energy $\hbar\omega$ to one of the momentum states of the outgoing (f) particle at the same energy, namely (Büttiker *et al.*, 1985)

$$\mathcal{T}(\omega) = \sum_i \sum_f T_{if}(\omega) = \mathrm{Tr}\{\tau\tau^\dagger\}, \tag{7}$$

where τ is a submatrix of the scattering matrix with dimensions $N_R \times N_L$, with N_R and N_L the number of channels in the right and left leads, respectively, at energy $\hbar\omega$. This result can be cast in another equivalent form in terms of single-particle Green's functions via (Meir and Wingreen, 1992)

$$\mathcal{T}(\omega) = \mathrm{Tr}\{G^r \Gamma_L G^a \Gamma_R\}, \tag{8}$$

where $G^{r(a)}$ is the retarded (advanced) single-particle Green's function corresponding to the interaction of a "central" part of the junction with the electrodes, and $\Gamma_{L(R)}$ describes the "rate" at which particles scatter between the leads and the central part of the junction. It has been rederived for thermal transport by many (Ozpineci and Ciraci, 2001; Mingo and Yang, 2003; Segal *et al.*, 2003; Mingo, 2006; Wang *et al.*, 2006; Yamamoto and Watanabe, 2006; Galperin *et al.*, 2007a; Wang *et al.*, 2007; Dhar, 2008).

Arguably the most universal result obtained from the Landauer formula (6) is that of thermal conductance quantization. Similar to the quantization of electrical conductance in ideally one-dimensional (1D) electronic systems (van Wees *et al.*, 1988), at low temperatures the thermal conductance (per phonon mode) was predicted to acquire a quantized value

$$\sigma_0 = \frac{\pi^2 k_B^2 T}{3h}, \tag{9}$$

where h is Planck's constant (Pendry, 1983; Maynard and Akkermans, 1985; Greiner *et al.*, 1997; Rego and Kirczenow, 1998). This result is readily derived from Eq. (6) in linear response by setting the number of modes to unity and letting the transmission coefficient to be 1, i.e., $\mathcal{T}(\omega) = 1$.

The fact that this conductance is material independent relies on the fact that, as in the electronic case, in 1D the phonon density of states is exactly proportional to the inverse of the group velocity. Remarkably, thermal conductance quantization does not depend on the statistics of the carriers (Rego, 2001). Indeed, σ_0 was experimentally measured for phonons (Schwab *et al.*, 2000), electrons (Chiatti *et al.*, 2006; Nicholls and Chiatti, 2008), and even photons (Meschke *et al.*, 2006).

Another application of the Landauer formula (6) has been in the study of geometrical and temperature effects on thermal transport. To give a few examples, this approach has been used to understand the role of defects on the thermal conductance of a nanowire (Chen *et al.*, 2005a), the effects of different geometries such as stubs, T junctions, and concavities (Tang *et al.*, 2006; Peng *et al.*, 2007; Xie *et al.*, 2008), periodic modulations (Tang *et al.*, 2007), and surface roughness (Kambili *et al.*, 1999; Santamore and Cross, 2001). As a general rule, disorder and temperature are found to have competing roles: Disorder tends to reduce the thermal conductance (by decreasing the transmission coefficients of the different transport modes), and a temperature increase usually results in a larger thermal conductance, due to an increased number of modes which participate in the thermal transport.

The interplay between the two processes can result in interesting phenomena. For instance, Santamore and Cross (2001) showed that disorder in the form of surface roughness may generate a nonmonotonicity in σ_{th} with increasing temperature, with a slight decrease (below the quantum of thermal conductance) followed by a rise of σ_{th} with increasing temperature, similar to the experimental results of Schwab *et al.* (2000). Their results (shown in Fig. 3) are

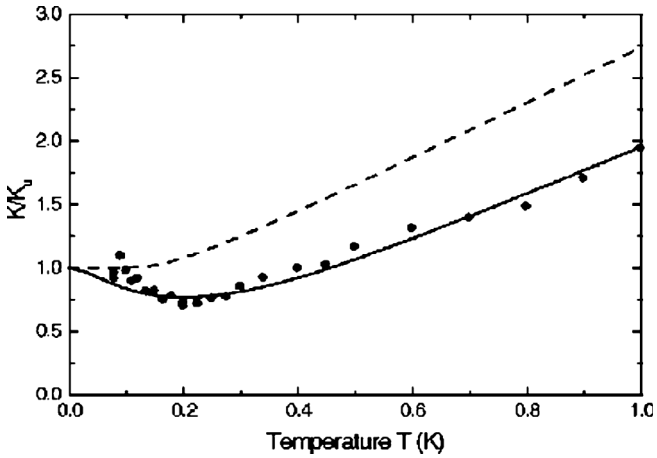

FIG. 3. Thermal conductance of a quasi-1D wire with surface roughness, exhibiting inhomogeneous thermal conductance. Points correspond to experimental data of Schwab *et al.* (2000), and the solid line is the theoretical curve. From Santamore and Cross, 2001.

explained as follows: At very low temperatures, there is only one mode which contributes to the thermal conductance. As temperature increases, scattering of that mode off the surface roughness increases, generating a decrease in the thermal conductance. As the temperature is raised even higher, higher modes start to participate in the thermal transport, giving rise to an increase in the thermal conductance.

This ties with the use of the scattering approach to thermal conduction in real materials, which comes about from using realistic phonon spectra (e.g., as obtained from experiment or first-principle approaches) in combination with ground-state density-functional theory (DFT) calculations to obtain the scattering coefficient $\mathcal{T}(\omega)$. To give several examples, Tanaka *et al.* combined geometrical structure (i.e., realistic shape of the wire) with real material parameters to study the onset of the thermal conductance quantization in GaAs and silicon nitride wires (Tanaka *et al.*, 2005). The thermal conductance of nanowires made of, e.g., Si, Ge, and GaAs was studied by several (Mingo and Yang, 2003; Mingo *et al.*, 2003; Tanaka *et al.*, 2005; Wang and Wang, 2007). Much attention has been given to carbon-based structures, such as carbon nanotubes, graphene, and graphite (Yamamoto *et al.*, 2004; Mingo and Broido, 2005a, 2005b; Zhang and Li, 2005; Yamamoto and Watanabe, 2006; Lü and Wang, 2008; Zimmermann *et al.*, 2008,; Lan *et al.*, 2009). Another example is the recent study of isotope and disorder effects (Murphy and Moore, 2007), specifically in carbon and boron-nitride nanotubes (Savić *et al.*, 2008a, 2008b; Stewart *et al.*, 2009).

Some universal conclusions arise from these calculations. For instance, a dimensional crossover from three- to one-dimensional transport (manifested by, e.g., a change in the temperature dependence of the thermal conductance) occurs in many systems as the diameter of the nanotube decreases, and the length scales are determined by the wavelengths of the typical phonon modes (Wang and Wang, 2007). Also, disorder in various forms (local defects, surface roughness, etc.) has a dramatic effect on the thermal conductance, as it influences the scattering of the different modes (Roy and Dhar, 2008). Because of the translational invariance of the lattice, long wavelength (or zero-frequency) modes are always conducting, while short wavelength modes are scattered by disorder. Since the short wavelength modes participate in the thermal transport only at high temperatures, it is found that the low-temperature thermal conductance is less affected by disorder and defects. Finally, the thermal conductance of molecular junctions has also been widely studied (Segal *et al.*, 2003; Mingo, 2006; Galperin *et al.*, 2007a). It is found to be strongly dependent on a multitude of factors, among which are the phonon spectrum of the molecules, the degree of localization of the molecular modes, the molecule-lead coupling, nonharmonicity (i.e., phonon interactions), etc.

It is important to stress again that Eqs. (6)–(8), and indeed the whole Landauer approach, are based on some strong assumptions, which may break down in nanoscale junctions and under certain experimental conditions. The first assumption is that the system is ''closed,'' in the sense that it does not dynamically interact with its environment. The latter only provides the boundary conditions and the relevant parameters (such as the temperatures, chemical potentials, etc.). The second assumption is that the leads are ideal, i.e., are unaffected by the proximity to the junction (either in their structure or in the distribution of particles) and support well-defined single-particle states. In addition, it is assumed that ''dissipation'' takes place at the (infinitely far) edges of the leads and that the temperature (and chemical potential for electrons) is uniform in them. Most critically, the approach does not provide information on the *dynamics* of the system. Therefore, transient, memory, and nonlinear dynamical phenomena are beyond its reach. A further issue arises when one uses ground-state DFT in combination with the Landauer approach: One is effectively using a ground-state theory for a nonequilibrium problem. This issue cannot be solved by knowledge of the exact ground-state exchange-correlation functional, and as such, the use of ground-state DFT in this context can only be viewed as a mean-field approximation. This has been explicitly demonstrated by Vignale and Di Ventra (2009), where for the case of electrical conductance it was shown that the exact resistivity tensor $\overleftrightarrow{\rho}$ can be written as

$$\overleftrightarrow{\rho} = \overleftrightarrow{\rho}_s + \overleftrightarrow{\rho}_{xc}, \tag{10}$$

where $\overleftrightarrow{\rho}_s$ is the resistivity tensor of a noninteracting system in the presence of a static potential V_s that reproduces the *exact* ground-state density, and $\overleftrightarrow{\rho}_{xc}$ is a dynamical contribution related to dynamical exchange-correlation effects, and which does not vanish even in the zero-frequency (dc) limit. A possible way out would be to use a fully dynamical approach [e.g., the microcanonical picture of transport as suggested by Di Ventra and Todorov (2004)] combined with time-dependent DFT (Runge and Gross, 1984). This approach [recently implemented to study charge transport (Cheng *et al.*, 2006)] would provide, in principle, the exact thermal total current, if the exact dynamical exchange-correlation potential is known. However, we are not aware of any calculation of thermal current along these lines.

2. The role of interactions

Up to this point the system Hamiltonian has been assumed to describe single particles with interactions included at most at the mean-field level. As mentioned above, many-body correlations can be accounted for within a time-dependent DFT approach, namely, within an effective single-particle picture. Alternatively, the effect of interactions beyond mean field could be explicitly included via the so-called nonequilibrium Green's functions formalism (NEGF) [see, e.g., Mingo, Chapter 3 in Volz (2009)]. In this approach one solves equations of motion for appropriate single-particle Green's functions that can be conveniently defined on the Keldysh contour (Kadanoff and Baym, 1962; Keldysh, 1964). In its exact formulation, the NEGF has however limited practical utility, since, if one assumes particles interacting—beyond mean field—in the *whole* system (leads plus nanostructure), no closed equation of motion for the single-particle Green's functions can be obtained (Di Ventra, 2008). Instead, it is common to assume (as in the Landauer approach) that the leads contain noninteracting particles and interactions are confined within a central region containing the nanostructure. This is a strong assumption and

may not always correspond to the physical problem at hand and/or its experimental realization.

If one makes the assumption of noninteracting particles in the leads, and assumes that a steady state has been reached in the long-time limit (not an obvious statement either), the equation of motion for the different single-particle Green's functions can be closed and the NEGF provides a compact expression for the total current similar to that derived for electron transport (Meir and Wingreen, 1992), given by

$$J = \frac{1}{4\pi}\int_0^\infty \hbar\omega d\omega[(G^r - G^a)(\Sigma_R^< - \Sigma_L^<) + +iG^<(\Gamma_R - \Gamma_L)], \tag{11}$$

where $G^{r,a,<}$ are the retarded, advanced, and "lesser" single-particle Green's functions, respectively; $\Sigma_\alpha^<$ are the lesser self-energies of the $\alpha = L, R$ leads, and $\Gamma_\alpha = i(\Sigma_\alpha^r - \Sigma_\alpha^a)$, namely, the difference between "retarded" and "advanced" self-energies (the explicit ω dependence of all these quantities has been omitted). The first term on the right-hand side of Eq. (11) may be interpreted as describing the current from the bias-induced difference in the coupling to the leads, while the second is related to the nonequilibrium distribution function in the interacting region. The single-particle Green's functions can represent either phonons or electrons and should be calculated in the presence of interactions. In the mean-field approximation, Eq. (11) reduces to Eq. (6) (or its equivalent form for fermions). Many-body perturbation expansions to compute these Green's functions have been performed for simple model Hamiltonians (Galperin *et al.*, 2007a; Lü and Wang, 2007), but it is no easy task to introduce interactions (beyond mean field) in realistic systems.

The NEGF could also be used to study the effects of electron-phonon interactions. In that case as well, however, quite strong approximations need to be made in order to have an analytically tractable theory. For instance, if one assumes electrons interacting with each other at a mean-field level, but interacting in a central region with noninteracting phonons, the heat current can be approximated as a sum of contributions from both electrons and phonons, $J = J_{el} + J_{ph}$, where each component is calculated with the help of Eq. (11). The key ingredient here is that, due to the electron-phonon interaction, the self-energy of phonons includes an electronic contribution and vice versa. These contributions can be calculated in a perturbative way. However, this is clearly an idealization, since it neglects correlated electron-ion motion, which, in principle, does not even allow the total thermal current J to be separated into two distinct contributions from the two particle species. Along the same lines of reasoning, the effects of phonon-phonon interaction have been studied (Liu and Yi, 2006; Mingo, 2006; Xu *et al.*, 2008). According to these results both electron-phonon and phonon-phonon interactions decrease the thermal conductivity. However, we need to stress again that due to the large current densities nanoscale systems carry—and hence the large number of scattering events per unit time and unit volume—it is not a simple task to include all the relevant physical scattering mechanisms in the present nonequilibrium case. An example of this is the possibility of phonon modes in the junction which are weakly coupled to the bulk modes of the electrodes. In this case, these "localized" modes may be energetically "pumped" by scattering with electrons or other phonons before energy could efficiently be dissipated away. This physical situation is beyond second-order perturbation theory and more work in this direction is thus highly desirable.

3. Molecular dynamics

Another method to evaluate the thermal conductivity which is gaining increasing popularity is that of molecular dynamics (MD). Basically, molecular dynamics comes down to solving the classical equations of motion of the system numerically. The origin of the method in the present context can be traced back to the seminal work of Fermi, Pasta, and Ulam (1955), where the energy transfer in nonharmonic lattices has been studied numerically. Since then it has been widely used to study heat transport in classical 1D systems (Lepri *et al.*, 2003; Dhar, 2008). It has also been generalized to study quantum effects by providing appropriate boundary conditions (Wang *et al.*, 2008). These approximations, however, should be thought of as quasiclassical, since the microscopic dynamics of the system is described by classical Newtonian equations of motion, and the quantum nature is only introduced via indirect conditions (such as the noise in a Langevin term). An advantage of molecular dynamics is the ability to model realistic systems and geometries in a rather straightforward way. The forces between atoms are evaluated from realistic parameters, so that different geometries, impurities, structures, etc., are easily taken into account.

In order to calculate the heat transport directly from MD, one needs to account for a finite temperature in the system. This is usually done in a linear response by adding to the Newtonian equations of motion a Langevin fluctuating term which satisfies the fluctuation-dissipation relation, i.e., the two-time correlation function of the current is proportional to the temperature [see, e.g., Van Kampen (2001)]. Alternatively, a Nosé-Hoover thermostat is introduced in which a fictitious coordinate is added to the real coordinate to maintain a finite temperature (Nosé, 1984; Hoover, 1985).

Once a finite temperature is set, there are two main methods to calculate the thermal conductivity. The first (sometimes called equilibrium MD) is via the linear-response Green-Kubo formula (Luttinger, 1964; Lepri *et al.*, 2003; Dhar, 2008)

$$\kappa = \frac{1}{3Vk_BT^2}\int_0^\infty \langle J_{th}(t)J_{th}(0)\rangle dt, \tag{12}$$

where V is the volume, k_B is the Boltzmann constant, T is the system temperature, $J_{th}(t) = \int d\mathbf{r} j_{th}(\mathbf{r}, t)$ is the integral of the heat current density $j_{th}(\mathbf{r}, t)$ over the entire system, and the brackets denote equilibrium ensemble averaging in the absence of a thermal gradient. However, the Green-Kubo equation has two main weaknesses. The first is that it is derived in the thermodynamic limit and therefore its use in finite systems is not well justified (Kundu *et al.*, 2009). Second, one needs to assume that a small temperature gradient (the external perturbation) ensues in the system, which may not be the case in every experiment. However, its relative simplicity makes it a good starting point in many cases.

An alternative method (also known as nonequilibrium MD), still based on molecular dynamics, is the one in which

the system is held in contact between two heat baths of different temperatures. Once the dynamics reaches a steady state, the temperature profile and the local heat currents can be calculated, from which the thermal conductivity is extracted. Here lies one of the disadvantages of the model, since the definition of the local heat current requires defining a local energy operator, which is not always a unique quantity (Lepri *et al.*, 2003; Wu and Segal, 2009). Likewise, a local temperature needs to be defined and evaluated, a somewhat tricky issue to which we will return to in Sec. III. At high temperatures (where the distribution function is practically classical and quantum effects are negligible, say at temperatures higher than the typical vibrational mode temperature) one may define the local temperature as the kinetic energy of the atoms (via the equipartition function), but this assumption breaks down at low temperatures, and one needs to use a definition of temperature which rests on the equilibrium distribution of phonons (Wang *et al.*, 2008). This yields a quasiclassical treatment (which is somewhat better than a fully classical treatment at low temperatures), but leans on the assumption that the phonon distribution resembles its equilibrium form, which may not be the case in this nonequilibrium problem. On the other hand, the obvious advantage of this method is that it does not rely on any thermodynamic-limit assumptions and is thus applicable for any system size, which is important for the study of realistic nanoscale systems. For instance, Yang *et al.* (2010) recently used the method to study Fourier's law and thermal conductance of realistic Si nanowires and showed that Fourier's law breaks down in these systems (see Sec. III.D). Studies along similar lines have recently been performed to investigate the thermal conductance of carbon nanotubes (Berber *et al.*, 2000; Padgett and Brenner, 2004; Hu *et al.*, 2008), Si wires (Ponomareva *et al.*, 2007; Henry and Chen, 2008b; Yang *et al.*, 2008), diamond nanorods (Padgett *et al.*, 2006), and polyethylene chains (Henry and Chen, 2008a), to name only a few recent studies.

An additional method, related to MD, is that of *lattice dynamics* models. In this method the phonon dispersion relations are obtained by calculating the direct change in energy due to atom displacements, using force fields obtained from DFT calculations (Feldman *et al.*, 2000; Ren *et al.*, 2006; Turney *et al.*, 2009).

The abundance of literature makes it hard to describe universal features of the thermal conductance, which seems to strongly depend on the details of the model and/or material. Specifically, σ_{th} is very sensitive to the phonon spectra and to phonon localization (Zhernov and Chulkin, 2000; Dhar and Lebowitz, 2008), which are in turn sensitive to material, geometry and disorder, surface roughness, and more. The rationale behind these studies is that by uncovering the detailed influence of these parameters on σ_{th}, theory may provide guidance to experiments and even suggest new materials with optimized thermal properties.

III. LOCAL TEMPERATURE AND HEATING

A. General remarks

When a current passes through a classical resistor, the latter heats up. This phenomenon is known as "Joule heating." It is a consequence of the inelastic relaxation of electrons in the resistor which transfer energy to the surrounding lattice (Ashcroft and Mermin, 1976). In a nanoscale system, such as a molecular junction or an atomic wire, electrons can analogously scatter inelastically off the phonons (i.e., the vibrational modes of the structure). However, since electrons typically spend very little time in the junction region, one might naively think that their inelastic scattering rate is negligible with consequent little heating of the junction itself. This conclusion, which is, for instance, at the heart of the Landauer scattering approach where all dissipation is assumed to occur only in the "reservoirs," does not take into account the fact that due to the small cross section of nanoscale systems, the *current density* at the junction can be very large (typically much larger than in mesoscopic and macroscopic systems, see footnote 2). This implies that the power *per atom* in the junction can be very large, possibly leading to large local heating (Todorov, 1998; Chen *et al.*, 2003, 2005b). The rate at which this power is then dissipated back to the electrodes determines the effective local (and out of equilibrium) temperature of the junction.

In addition, current-carrying electrons can transfer energy, via inelastic electron-electron interactions, to other electrons in the Fermi gas (D'Agosta *et al.*, 2006). This effect is generally small in macroscopic systems. However, similar to the increased rate of electron-phonon scattering in nanoscale junctions due to the large current densities, the inelastic scattering rate of electron-electron interactions may increase in nanoscale systems leading to a local heating of the electron liquid (D'Agosta *et al.*, 2006). This effective higher temperature of the electrons may influence the local ionic heating due to electron-phonon interactions and thus can be indirectly measured by measuring the local temperature of the ions or the broadening of inelastic conductance features (D'Agosta and Di Ventra, 2008a).

An obvious reason why local temperatures and heating are such important phenomena lies in the fact that substantial heating of a nanoscale system leads to the system instability and eventually to the breaking of atomic bonds (Teramae *et al.*, 2008; Tsutsui *et al.*, 2008b; Ward *et al.*, 2008). A different and even more fundamental interest in these phenomena arises in the context of Fourier's law, Eq. (1), that we will discuss in Sec. III.D. Of course, at the nanoscale, it seems inappropriate to discuss the scaling of the thermal conductance with length, since this is an asymptotic (in terms of system size) property (Lepri *et al.*, 2003). Thus, one is left with the simple question: Under which physical conditions does a uniform temperature gradient develop in a nanoscale system held in contact between two heat baths of different temperatures?

In this section we discuss all these issues. We review the various mechanisms which give rise to heating in current-carrying junctions, using simple arguments and models, followed by some basic results obtained from more elaborate models. We then turn to a discussion of the onset of a temperature gradient, analyzing a molecular wire junction in terms of the theory of open quantum systems, discussed in some detail in Sec. IV.C.2.

B. Heating in current-carrying nanostructures: Theory

1. Various definitions of out-of-equilibrium temperature

In order to discuss local heating, the first question one should ask is how is a local temperature defined and calculated? Since temperature is a thermodynamic quantity, some caution is needed (Hartmann *et al.*, 2004a, 2004b; Hartmann and Mahler, 2005). Apart from the definition of temperature that we have given in Sec. II.A, and which we will also use in Sec. III.D, we report here on several other notions of local temperature (not necessarily leading to the same quantitative results) and their microscopic origin, which were used to study local ionic heating in atomic junctions, each with its own pros and cons.

Kinetic definition.—An intuitive definition of local temperature is to relate it to the local kinetic energy of the ions, i.e., $\langle(1/2)mv^2\rangle \sim 3k_BT/2$. However, this definition, mainly used in molecular dynamics simulations (see Sec. II.C.3), has several drawbacks: (i) It relies on the equipartition theorem which is strictly proven in the thermodynamic limit only for systems whose energy is quadratic in the particle momenta (as for noninteracting systems) and does not encompass any quantum effects. (ii) One needs to define an average kinetic energy over some length scale, while the quantum nature of particles may preclude such a definition.

Local phonon mode.—Consider a phonon mode somehow coupled to the system and vary its temperature in such a way that no heat flows between that mode and the system. This idea is somewhat similar to the idea of connecting an external bath to a system and imposing the restriction that no heat current flows between the system and bath, which was suggested by the study of the onset of Fourier's law in one-dimensional systems, both classical and quantum (Bonetto *et al.*, 2004; Dhar and Roy, 2006; Dhar, 2008; Roy, 2008). This idea was recently used to study the local temperature of a model molecular junction using the NEGF formalism (Galperin *et al.*, 2007a, 2007b). The main result is the existence of two voltage thresholds. The first is at the voltage that corresponds to the vibrational energy of the phonon, $eV \sim \hbar\omega_0$, at which local heating starts to occur and the temperature increases abruptly. The local temperature then remains roughly constant, until it rises again when the bias is so large as to encompass the molecular conduction window [i.e., both the highest occupied molecular orbital (HOMO) and the lowest unoccupied molecular orbital (LUMO) states]. The disadvantage of this method is that the temperature of the mode depends on the microscopic details, i.e., the phonon excitation energy $\hbar\omega_0$ and/or the electron-phonon coupling.

Distribution function definition.—A slightly different model of local temperature is to connect a phonon mode to the nanoscale system, but instead of determining its temperature self-consistently, its distribution function is compared to an equilibrium distribution function with a given temperature, which is tuned to give the best comparison. Clearly, the disadvantage of this method is that the nonequilibrium distribution function may be very different from the equilibrium one (Pekola *et al.*, 2004; Koch *et al.*, 2006). The last two methods were compared and were found to give similar local temperatures at large bias (compared to the typical vibrational modes, implying strong nonequilibrium and population of higher modes), but deviated from each other substantially at low biases. In fact, the second method turned out to give erroneous results in the zero-bias limit, when one expects the temperature to be the same as that of the leads. This is precisely because an equilibrium form for the phonon mode was assumed, although even with no current the distribution function of the mode may have contributions arising from the coupling to the electronic (and other phononic) degrees of freedom in the junction (Galperin *et al.*, 2007a).

Definition from dissipated power.—A microscopic theory which relies on first principles was suggested by Chen *et al.* (2003, 2005b). The method is as follows. As a starting point, the electronic scattering states are calculated using ground-state DFT. The electron-phonon coupling for the different modes is also calculated using first-principles approaches. Using perturbation theory one can then calculate the power dissipated into the junction from current-carrying states. This power is then compared to the rate at which heat escapes the junction, typically assumed as $\sigma_{th}T^4$, with σ_{th} the thermal coefficient that can be estimated from a microscopic model and T the effective temperature of the junction (Chen *et al.*, 2003, 2005b). A result of these calculations is shown in Fig. 4, where the local temperature as a function of bias was calculated for a benzene-dithiol (BDT) junction and a gold-atom point contact. The results indicate that, for a given bias, the BDT junction heats up less than the gold-atom junction, due to better thermal coupling with the electrodes and larger resistance to electrical currents [see Eq. (13)]. This result is also confirmed by experiments on similar systems (Huang *et al.*, 2006; Tsutsui *et al.*, 2007; Teramae *et al.*, 2008). While not visible from Fig. 4, theoretical results of the threshold voltage for heating [see Eq. (13)] are also in good agreement with experiments (Chen *et al.*, 2003, 2005b). The same method was used to study local heating in alkane chains of different lengths (Chen *et al.*, 2005b). It was predicted that, at fixed voltage, heating decreases with increasing chain length, which is due to increased resistance to electron flow, a result also confirmed experimentally (Huang *et al.*, 2007). More recently, the same approach was used to study the effect

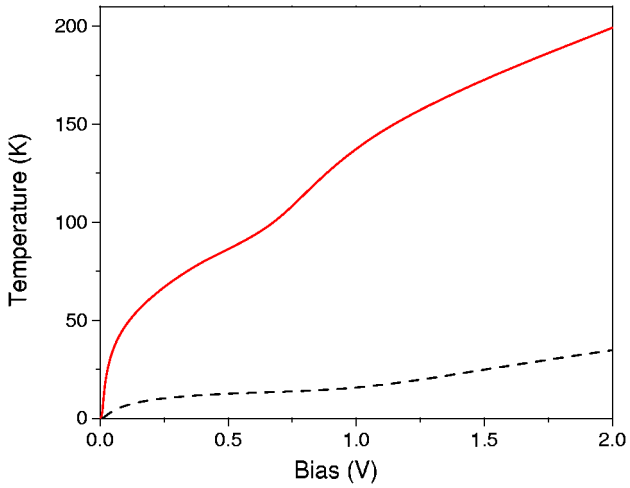

FIG. 4 (color online). Local temperature as a function of bias, calculated from a scattering theory approach, for a benzene-dithiol molecular junction (dashed line) and a gold-atom point contact (solid line). From Chen *et al.*, 2003.

of different isotope substitutions on the heating in hydrogen molecular junctions (Chen, 2008). It was found that local heating is very sensitive to isotope effects since the electron-phonon coupling constant is inversely proportional to the ionic mass.

The method described above has the advantage that it can treat realistic systems. However, its main drawback is that it relies on the assumptions of the Landauer approach [see Sec. IV.C.1] and its practical implementation employs ground-state DFT, which, as discussed at length in this Colloquium, does not properly take into account all dynamical effects.

2. Ionic heating

After discussing various definitions of local temperature, we are now in a position to discuss local heating. As described previously, we consider here a junction, composed of leads (which are assumed to be held at local equilibrium), and a nanoscale system which has both electronic and vibrational degrees of freedom. Even in the presence of a current, we can assume that in the leads, far away from the nanojunction, electrons and phonons reach the same temperature T_0.[5] In the junction, however, the electrons and phonons may have different temperatures, T_e and T_{ph}, respectively. These temperatures depend on bias, strength of electron-phonon and electron-electron interactions, the coupling of phonons with the bulk phonons in the leads, as well as the transmission properties of the electrons.

We start by discussing the temperature of the ions in the junction, or the phenomenon of *local ionic heating* (see Fig. 5). We start from some simple considerations, assuming first that no inelastic electron-electron scattering occurs (Todorov, 1998; Di Ventra, 2008). The power of the entire circuit (nanojunction plus power source) is given by V^2/R, where V is the source bias and R is the junction resistance (assuming zero impedance of the external circuit). Only a small fraction α of this power, i.e., $\alpha V^2/R$, is dissipated into the ionic degrees of freedom in the junction due to the electron-phonon coupling. The value of α needs to be determined from a microscopic theory (Todorov, 1998). Since the spectrum of modes of the junction is typically discrete, one expects a minimal bias (we call V_c) necessary to excite the lowest-energy phonon mode of the structure, and hence $\alpha(V < V_c) = 0$.[6] Therefore we write $P = \Theta(V - V_c)\alpha V^2/R$, where Θ is the step function. Now, if the power P were not dissipated away from the junction, the latter would heat up substantially and eventually break down. Therefore, there must be a heat current I_Q which dissipates this power into the electrodes. Since the leads are much bigger than the junction and are three dimensional in nature, one can assume that this energy is carried away at a bulk rate $I_Q = \sigma_{th} T_{\rm eff}^4$ (Ashcroft and Mermin, 1976), with $T_{\rm eff}$ an average effective temperature of the junction ions and σ_{th} the lattice thermal conductance. At steady state the condition $P = I_Q$ then yields for the effective temperature

$$T_{\rm eff} = \Theta(V - V_c)\left(\frac{\alpha}{\sigma_{th} R}\right)^{1/4} \sqrt{V}. \tag{13}$$

Here we have considered the bulk electrode temperature $T_0 = 0$. If both electrodes are at finite temperature, then there is also a heat current $\sim\sigma_{th} T_0^4$ flowing into the junction, and hence the balance equation $P = I_Q^{\rm out} - I_Q^{\rm in}$ gives $T_{\rm eff} = (T_0^4 + T_V^4)^{1/4}$, where $T_V = \Theta(V - V_c)(\alpha/\sigma_{th} R)^{1/4}\sqrt{V}$ is the contribution to the temperature from the finite voltage bias.

In the above considerations we have assumed that heat can be dissipated away from the junction rather easily. The results may change depending on the heat-transport properties of the leads and the coupling between the leads and the junction. For instance, if the leads are strongly disordered, heat is carried away with a different exponent of the temperature difference (Yudson and Kravtsov, 2003). If the nanojunction has poor thermal coupling to the leads, or in the presence of localized phonon modes (Lepri *et al.*, 2003), namely, modes that have a very weak coupling with the bulk modes, then the local ionic temperature can reach very large values, even at relatively small biases. The reason is simple: In the above cases, due to the bias V, the current-carrying electrons are away from their ground state, and they are thus "seen" by the local modes of the nanostructure at an effective finite temperature. Thus, this situation provides the possibility for inelastic electron-ion scattering in an energy window $\sim$eV, with consequent ion temperatures of the same order of magnitude (Todorov, 1998; Yang *et al.*, 2005; Di Ventra, 2008). We note that similar results were recently obtained from microscopic considerations (Mozyrsky *et al.*, 2006). That being the case, a voltage bias of 0.1 V would generate an effective temperature of $\sim$1000 K. This seems to have been observed in atomic quantum point contacts at the breaking point (Ward *et al.*,

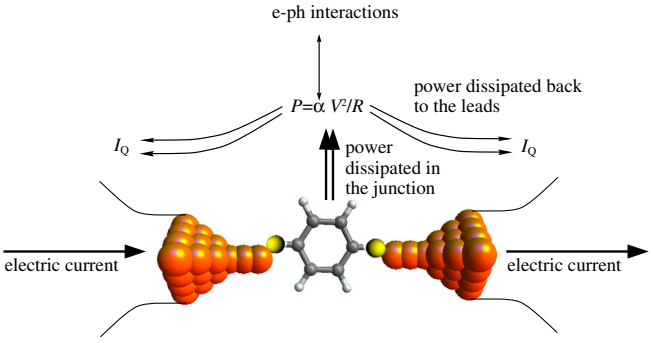

FIG. 5 (color online). A schematic representation of the mechanism of ionic heating in nanoscale junctions. The electric current dissipates a fraction $\alpha V^2/R$ of its power in the junction, depending on the strength of the electron-phonon interaction. This power is then dissipated to the phonons in the electrodes in the form of a heat current. The balance between the power flowing into the junction and the heat current I_Q flowing out of the junction determines the ionic temperature of the junction.

[5]The extent to which this statement is correct depends on the current density in the leads. If this current density can be assumed to be zero, then the leads are at an ideal global thermal equilibrium, with electrons and ions sharing the same temperature. Otherwise some difference (albeit extremely small) may arise between the lead temperature of the ions and electrons.

[6]In molecules, this bias may be very close to zero, due to the longitudinal "acoustic" mode of the whole molecule vibrating against the bulk electrodes.

2008). Thus, good thermal coupling to the electrodes is essential for maintaining junction stability.

3. Electron heating

Up to now we have discussed the heating of the phonons in the junction due to their interaction with the current-carrying electrons. But what about the temperature of the electrons themselves? To be precise, we refer here to the temperature T_e of the Fermi sea of electrons of the nanojunction and those in its proximity. This temperature is affected by both inelastic electron-electron interactions and electron-phonon coupling (D'Agosta *et al.*, 2006). Clearly, the local electron temperature influences the local ionic temperature of the junction. However, accounting for both electron-electron and electron-phonon interactions is a challenging task. While attempts have been made to account for both in calculating charge transport (Galperin *et al.*, 2007b) and recently even heat currents (Liu *et al.*, 2009a), we are unaware of any calculation of the local temperature where these interactions are considered on equal footing.

In a recent work, D'Agosta *et al.* (2006) predicted the bias dependence of the local electron temperature in quasiballistic nanoscale junctions and its effect on ionic heating, treating the electron liquid as a viscous fluid. The general argument, which was accompanied by a microscopic theory based on the quantum hydrodynamic equations for the interacting electron liquid (D'Agosta and Di Ventra, 2006), is as follows. Assuming no electron-phonon interaction is present, to first approximation, the thermal electronic conductance of the electron liquid can be taken to be proportional to the temperature, $\sigma_{th} = \gamma T_e$. Therefore, the heat current, given by $I_Q = \sigma_{th} T$, is quadratic in temperature, $I_Q = \gamma T_e^2$. As in the case of local ionic heating, at steady state this thermal current has to balance the power dissipated in the junction, which is a small fraction of the total power of the circuit, $P = \alpha V^2/R$. One thus obtains

$$T_e = \gamma_{e-e} V, \tag{14}$$

where γ_{e-e} is to be determined from a microscopic calculation. Assuming the coefficient γ_{e-e} is weakly dependent on bias, this simple argument shows that the local electron temperature grows linearly with bias. This result clearly hinges on the assumption that electronic heat is dissipated away from the junction at a bulk rate, which may not hold for all systems and under all experimental conditions.

From a microscopic hydrodynamic theory D'Agosta *et al.* (2006) also calculated the local temperature profile $T_e(x)$ along the junction. From the maximal value of T_e, an estimate of γ_{e-e} was supplied for various junctions. For instance, for a 3D gold quantum point contact (QPC) with effective cross section of 7 Å^2, they evaluated $\gamma_{e-e}(\mathrm{QPC}) = 65$ K/V. For a two-dimensional electron gas (2DEG), assuming a cross section of 20 nm they found $\gamma_{e-e}(\mathrm{2DEG}) = 1.2 \times 10^2$ K/V, suggesting that heating from inelastic electron-electron interactions is generally smaller than the corresponding heating due to an electron-ion interaction.

4. Ionic cooling

A direct measurement of local electron temperatures, however, seems a difficult task, and in fact we are not aware of such a direct method. On the other hand, local ionic temperatures are relatively easier to obtain (see Sec. III.C). It is then relevant to ask what is the effect of the local electronic temperature on the ionic heating. Since part of the total power dissipated in the junction goes into heating electrons via electron-electron interactions, that power is no longer available to induce ionic heating. Since the initial energy is always that of the current-carrying electrons, the ionic temperature must be smaller if electron heating takes place. The power of this electron-phonon scattering process can be assumed to have a form $P_{e-ph} = \Sigma(T_{ph}^n - T_e^n)$, with Σ a system-specific constant and $n > 0$ (Schmidt *et al.*, 2004). This ionic energy is then dissipated away from the junction. If we assume again a bulk dissipation law $I_Q = \sigma_{th} T_{\mathrm{eff}}^4$, for electronic temperatures much smaller than the ionic ones, the steady-state condition $P_{e-ph} = I_Q$ is satisfied by $\Sigma \sim \sigma_{th}$ and $n = 4$. By taking into account a background temperature T_0 we then get (D'Agosta *et al.*, 2006)

$$T_{\mathrm{eff}} = (T_0^4 + \gamma_{e-ph}^4 V^2 - \gamma_{e-e}^4 V^4)^{1/4}, \tag{15}$$

which is valid for $V < (\gamma_{e-ph}/\gamma_{e-e})^2$. The meaning of Eq. (15) is that at sufficiently large biases, the effective phonon temperature is reduced, i.e., the phonons "cool down." As we will discuss in Sec. III.C, this result has recently been confirmed experimentally (see Figs. 7 and 8). It is important to point out, however, that the exact power-law dependence in Eq. (15) and the value of the various coefficients may depend strongly on the details of the nanostructure and its contact with the leads.

Another interesting idea to obtain reduced ionic heating is to use a nanostructure with an appreciable Peltier coefficient. In this situation passing current through the junction would result in the cooling of one side of the junction, which may induce cooling of the molecule. The idea of local cooling of a junction has received renewed attention in recent years in the context of mesoscopic systems (Giazotto *et al.*, 2006; Saira, *et al.*, 2007) and molecular junctions (McEniry *et al.*, 2002; Galperin *et al.*, 2009b; Pistolesi, 2009; Zippilli *et al.*, 2009). While the details vary, the main concept is the same: The system is tuned in such a way that hot electrons (i.e., those with large kinetic energy) find it easier to tunnel through the junction, thus depleting the lead upstream in voltage from hot electrons, and thus cooling it. The cooling of the molecule is achieved either by its proximity to a cooler lead or, in more subtle cases, by the fact that electrons "borrow" energy from the localized phonon modes to assist transport, thus cooling them in the process (Galperin *et al.*, 2009b).

C. Heating in current-carrying nanostructures: Experiment

Despite the difficulty in directly measuring local temperatures of nanoscale systems, we have witnessed much progress in this direction over the past years. The first concepts of local temperature measurements are reviewed by Cahill *et al.* (2003). Especially noteworthy are experiments where a thermocouple (serving as a thermostat) is mounted on top of an STM tip, thus creating a "scanning thermal microscope" (SThM). This device was then used to study the local temperature of a carbon nanotube placed on a substrate (see

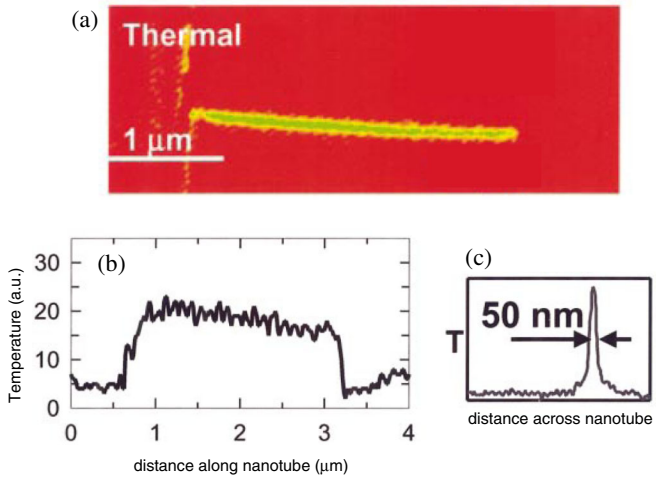

FIG. 6 (color online). Scanning thermal microscopy (SThM) of a 10 nm diameter multiwall carbon nanotube. (a) Full thermal image. (b) A cut along the nanotube. (c) A cut across the nanotube. From Cahill *et al.*, 2003.

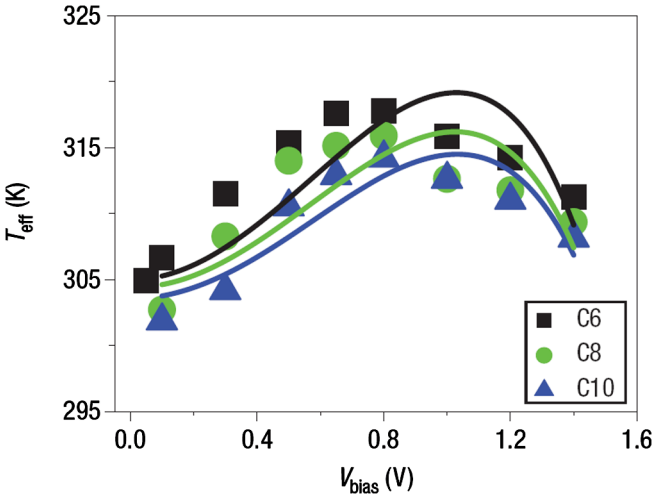

FIG. 7 (color online). Effective temperature of a molecular junction, for three different types of molecules *n*-alkanedithiol, with $n = 6$ (squares), $n = 8$ (circles), and $n = 10$ (triangles). The solid lines are theoretical estimates from Eq. (15). From Huang *et al.*, 2007.

Fig. 6). This work discusses several possible shortcomings and limitations of SThM studies: the dependence of the measured temperature on topography of the sample and surface chemistry, the fact that the tip itself might perturb the sample (e.g., via near-field radiation, or by effectively cooling it), only surfaces can be measured, some of the heat is delivered through the air between the sample and tip, etc. These issues render this method difficult for quantitative analysis, although some progress has been achieved (Grover *et al.*, 2006; Kim *et al.*, 2008). We are unaware of any theoretical work (other than the one presented here) which has been directly related to SThM measurements.

In mesoscopic systems (e.g., quantum dots etched in 2D electron systems) which are of typical sizes of microns, tremendous advance in local thermometry has been achieved, as summarized by Giazotto *et al.* (2006). In these systems, thermometry is achieved by analyzing some temperature-dependent function (current, conductance, etc.) from which, by using known properties of the electronic surroundings, the temperature can be extracted. To give a specific recent example, by analyzing the derivatives of the current as a function of temperature and voltage, Hoffmann *et al.* (2009) were able to measure the temperature gradient across a current-carrying quantum dot of 15 nm length, with the conclusion that the heat flow is mediated by phonons in the quantum dot.

Other options for measuring the local temperature are available. One method is to study the force at which a molecular junction breaks as a function of current. The idea behind this method is that the higher the temperature of the structure, the less external force is needed to break it (Huang *et al.*, 2007; Tsutsui *et al.*, 2008a, 2008b). From this force one can then extract an effective temperature. For example, Schulze *et al.* (2008) studied the breakdown of a molecular junction composed of a C_{60} molecule and directly showed that better cooling of the junction is achieved when the coupling between the molecule and the leads is improved.

Using the above method, in a recent series of experiments, Huang *et al.* (2006, 2007) studied the local temperature of single-molecule (alkanethiols) junctions as a function of voltage bias. Their results shown in Fig. 7 (points) indicate that with increasing voltage, the local temperature first increases, saturates, and then slightly decreases. This is in agreement with the prediction of Eq. (15) (solid lines), and suggests that electron-electron interactions indeed occur in these junctions. The same experiment also confirms that longer alkanethiol molecules heat up less due to increased electronic resistance, at fixed voltage (Chen *et al.*, 2005b).

An alternative method to study the local temperature has been suggested recently. It makes use of Raman spectroscopy and it was first applied to the study of a suspended nanotube (Bushmaker *et al.*, 2007; Deshpande *et al.*, 2009). In these measurements, the local temperature was deduced from the shifts in the local Raman G_+ and G_- bands of the nanotubes. They compared two nanotubes of lengths 2 and 5 μm, and found that the longer nanotube was less heated, an effect which was attributed to the thermalization of hot phonons at the center of the nanotube.

Along the same lines, the local temperature of a molecular junction has been investigated via Raman spectroscopy (Ioffe *et al.*, 2008). The idea is that the ratio between the Stokes and anti-Stokes intensities is directly related to their nonequilibrium populations in the presence of electronic current. The method has been discussed theoretically in detail (Ioffe *et al.*, 2008; Galperin *et al.*, 2009a). In Fig. 8 the effective temperature is plotted as a function of voltage bias, for different Raman modes. From the figure one can see that although the temperature is slightly different between different modes (due to the different electron-phonon coupling strengths and symmetries), the overall voltage dependence shows roughly similar features. Note also the apparent decrease in the local temperature, which is in line with the results of Huang *et al.* (2007). This study, along with the one described before, indicates that local Raman spectroscopy may serve as a valuable tool for the study of local temperatures at the nanoscale.

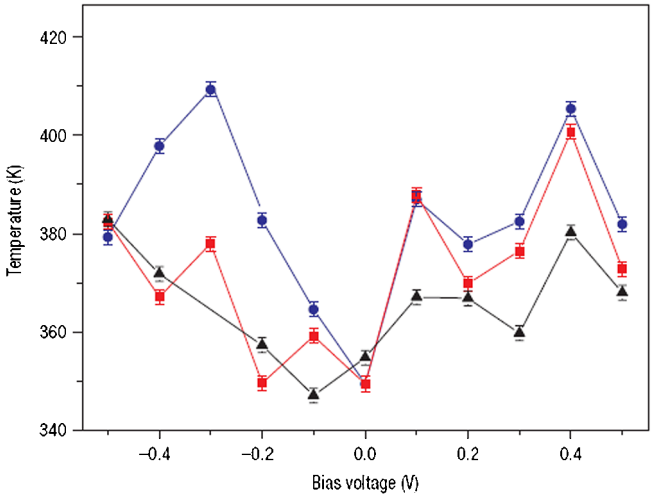

FIG. 8 (color online). Effective temperature of a molecular junction measured using Raman scattering. The different points correspond to different modes, and while the temperature is slightly different, the overall voltage dependence shows roughly similar features. Note also the apparent decrease in the local temperature with bias, which is in line with the results of Huang *et al.* (2007). From Ioffe *et al.*, 2008.

D. Fourier's law at the nanoscale

We end this section with a somewhat different issue, that of the onset of Fourier's law, Eq. (1), in nanostructures. As previously noted, in the context of nanoscale junctions there is not much point in discussing the scaling of the thermal conductivity κ, which pertains to an asymptotic relation, strictly valid in the limit of large system lengths. Therefore, here we limit our discussion to the simple question of what is the temperature profile along the junction.

In the context of Fourier's law, this question has been widely studied for both classical (Lepri *et al.*, 2003) and quantum systems (Michel *et al.*, 2006). The main focus has been on either spin chains (i.e., Ising-like models) (Michel *et al.*, 2006; Wu and Segal, 2008) or harmonic oscillator chains. The local temperatures are usually evaluated by calculating the averages of some local energy operators (Michel *et al.*, 2003; Saito, 2003; Michel *et al.*, 2006; Mejia-Monasterio and Wichterich, 2007), or by using self-consistent thermal baths (Dhar and Roy, 2006; Dhar, 2008; Roy, 2008; Jacquet, 2009). In the first case, one assumes that the local energy is related to the temperature via a local Boltzmann relation (Dubi and Di Ventra, 2009b), or directly proportional to the temperature via a local equipartition law (Michel *et al.*, 2003). The disadvantage of this method is twofold: (i) There is some arbitrariness in choosing the local energy operator, since one can represent the same Hamiltonian in different ways (Wu and Segal, 2009), and (ii) this method assumes from the outset that the system is in a local thermodynamic equilibrium, which may not always be the case.

In the second approach, the system is attached to local heat baths. The heat current between the junction (or quantum wire) and the local baths is calculated, and the temperatures of the heat baths are determined in such a way that the heat current between the wire and the baths vanishes. This method was recently described in detail and applied to a quantum chain of noninteracting harmonic oscillators (Roy, 2008) and a chain of quantum dots (Jacquet, 2009). For instance, Roy (2008) calculated, using quantum Langevin equations, the local temperature as a function of position for different chain lengths and for different coupling between the wire and the local baths. The conclusion of this work is that the coupling between the wire and the baths determines a length scale (mean-free path), and the heat transport crosses over from a diffusive regime (uniform temperature gradient) to a ballistic regime (uniform temperature, vanishing gradient) depending on the system length being longer or shorter than the mean-free-path, respectively. Since the dynamics of the system is calculated in the presence of the local baths, this shows that the properties calculated (i.e., local temperature) pertain to the combined system of quantum chain and thermal baths, and thus naturally depend on, e.g., the coupling strength between them.

Recently, a method was suggested to calculate the local temperature of electrons in a nanoscale junction (Dubi and Di Ventra, 2009c, 2009d). Its starting point is the stochastic Schrödinger equation [see Eq. (26)], which for noninteracting electrons reduces to a quantum master equation (Pershin *et al.*, 2008). In this approach the *finite* electronic system is coupled to two local heat baths at the edges of the system, similar to the study presented above for a chain of harmonic oscillators. In order to evaluate the local temperature, the definition introduced in Sec. II.A has been used. Namely, a third environment is coupled locally to the system at the position where the temperature needs to be evaluated. The properties of the system are then evaluated twice, once with the additional environment (the so-called "tip," as it mimics, e.g., the operation of a thermostat mounted on an STM tip) and once without the probe. The temperature of the probe is then varied (*floated*), such that a minimal change in some local (or global) properties of the system, such as its local electron density, occurs. A scan of the local temperature of the whole system can then be obtained with this method. The advantage of this approach is that it can, in principle, be implemented experimentally, and it provides the local temperature of the electrons without further scattering from other sources. In addition, it can be shown analytically that the above definition reduces to the standard thermodynamic temperature in limiting cases, for instance, in local equilibrium [see also Di Ventra and Dubi (2009)] or for two-level systems.

For the case of a wire coupled to two electrodes at different temperatures, it was found that the local temperature of the wire may exhibit quantum oscillations for intermediate lead-wire couplings (Dubi and Di Ventra, 2009d). Similar oscillations were later observed for a driven quantum wire (Caso *et al.*, 2010) and reflect the quantum coherent nature of the system. When the lead-wire coupling is large enough a uniform temperature ensues. In this limiting (ballistic) case, one also finds that the nonequilibrium distribution function of the system is an average of the distribution functions of the left and right baths. The fact that the temperature is uniform in the wire demonstrates the known result that for a clean system, Fourier's law is invalid.

In order to reconstruct Fourier's law (with an associated temperature gradient), diagonal disorder was introduced in the wire (which localizes the electronic wave functions), and the local temperature was averaged over disorder realizations (Dubi and Di Ventra, 2009c). It was found that for large enough disorder, a local uniform temperature gradient ensues, giving rise to Fourier's law. This result was interpreted in terms of an effective thermal length which controls the scale of the temperature gradient (Dubi and Di Ventra, 2009b). By adding the effect of dephasing, the model was also able to explain the results by Roy (2008) described above. We finally conclude that for the above model the onset of Fourier's law coincides with the onset of chaos (Dubi and Di Ventra, 2009c). This has also been found in other model systems (Michel *et al.*, 2006; Gaul and Büttner, 2007), but not in all cases (Lepri *et al.*, 1997; Li *et al.*, 2002). Thus, this result appears not to be universal.

IV. THERMOPOWER

A. Introduction and basic definitions

In this section we discuss the concept of thermopower in nanoscale junctions. As prototypical examples that show all main features of the problem we will be focusing mainly on experiments in molecular junctions (Reddy *et al.*, 2007) and briefly mention experiments in mesoscopic systems and nanowires. The thermopower phenomenon corresponds to the case in which a temperature difference at two sides of a given junction induces a voltage drop across it. From a technological point of view, this effect is of great importance, since it may be used to recover part of the heat wasted in physical processes and generate electrical power with no moving mechanical parts. It is also of basic scientific interest, since, by combining energy and charge flow, it may encode information about the system dynamics which is unavailable in charge transport experiments (Segal, 2005).

The configuration we have in mind is again a junction composed of two leads separated by a nanoscale element—a quantum dot, a molecule, nanotube, etc. Consider such a junction, where the two leads are held at different temperatures, T_L and T_R. The corresponding temperature difference $\Delta T = T_R - T_L$ gives rise to both a heat current (discussed in Sec. II) and a charge current. If the circuit is closed, after a transient time charges accumulate on one side of the junction and deplete on the other, so that a zero charge current is achieved and a voltage drop across the junction is formed. If the circuit is open (namely it is connected to an electron source), and a voltage difference ΔV is applied between the two leads with appropriate sign, a bias-induced electric current can cancel out the thermally induced current. Note, however, that given a temperature difference the two procedures may not yield the same voltage difference. In fact, the voltage difference may also depend on the location along the system where it is probed.

The thermopower S is defined as (minus) the amount of voltage ΔV at the state of vanishing current,

$$S = -\left.\frac{\Delta V}{\Delta T}\right|_{I=0}, \tag{16}$$

in the limit of $\Delta T \to 0$.

This definition can also be understood from the current expressed in linear response. This is defined as

$$I = G\Delta V + L_T \Delta T, \tag{17}$$

where G is the electrical conductance and L_T is a response coefficient related to the energy flow. From this expression one readily sees that $S = L_T/G$. Therefore, in order to determine S, one has to determine the conductance G and the thermal response L_T.

Before we proceed to discuss different theoretical and experimental aspects of the thermopower, it is important to ask the following question: Is knowledge of the thermopower S sufficient to design devices that operate as efficient heat-voltage converters? In fact, in a real device, it is not at all clear that the system is, under the given experimental conditions, in the linear-response regime. Nor it is obvious that the best conversion should be achieved in that regime (Dubi and Di Ventra, 2009d; Esposito *et al.*, 2009).

To this end, it is useful to define the unitless "figure of merit,"

$$ZT = \frac{GS^2}{\sigma_{th}/T}, \tag{18}$$

where T is the temperature of the system (Mahan and Sofo, 1996). The quantity ZT describes the efficiency of a real device or material as a thermoelectric converter. While an exact relation between ZT and thermodynamic efficiency is available (Müller, 2008), this choice can be intuitively understood: S measures how large a voltage drop can develop for a given temperature gradient, G measures how easy charges can cross the junction to generate that voltage drop, and σ_{th} measures how hard it is to maintain a temperature gradient.

It is commonly stated that for applications one must achieve $ZT \gg 1$ [in fact $ZT > 4$ would already be a great advance (Majumdar, 2004)]. However, such a situation is hard to obtain: In most cases the electrical conductivity σ and thermal conductivity κ are related via the Wiedemann-Franz law (Ashcroft and Mermin, 1976), which states that

$$\frac{\kappa}{\sigma} = \left(\frac{\pi^2 k_B^2}{3e^2}\right) T, \tag{19}$$

with the quantity in parenthesis commonly referred to as the "Lorenz number." This means that it is difficult to increase σ and S without also increasing κ, and vice versa. However, deviations from the Wiedemann-Franz law have been observed (Appleyard *et al.*, 2000) and discussed theoretically in various systems, including Luttinger liquids (Kane and Fisher, 1996; Li and Orignac, 2002; Rejec *et al.*, 2002; Kubala *et al.*, 2008; Murphy *et al.*, 2008; Garg *et al.*, 2009). These deviations are attributed to interactions, where the simple single-particle theory fails (see Sec. IV.C on theoretical methods), and are exactly what is required in order to increase the efficiency of thermoelectric devices.

B. Experiments on thermopower at the nanoscale

Measurements of thermopower are conceptually easier than those of thermal conductance: One applies a temperature gradient across the junction and measures the ensuing voltage

in a closed circuit when the transient current vanishes. Or, in an open circuit, one supplies a voltage to compensate for the thermally induced current. The slope of the resulting voltage-temperature gradient curve gives the thermopower. However, in an actual experiment, particular care needs to be taken to extract this quantity. The reason is because the voltage probe that is connected to the system in order to measure the thermopower is necessarily invasive, since the applied thermal gradient would induce, locally at the voltage probe contact, an extra voltage difference. This extra effect needs to be subtracted to get the actual thermopower of the nanojunction. In addition, the ensuing voltage (including its sign) is very sensitive to the junction geometry and thus may fluctuate considerably in an actual experiment, providing nontrivial distributions of the voltage as a function of thermal gradient, from which a single voltage value may not always be easy to extract.

Before reviewing some recent experiments on nanoscale junctions, it is of interest to briefly survey some of the older experiments on mesoscopic systems as well. We point out that while most of these experimental results may be understood in terms of a linear-response scattering theory (see Sec. IV.C), some recent results, such as the appearance of additional peaks in the distribution of induced voltages versus temperature gradient (Scheibner *et al.*, 2005), are yet to be completely accounted for. The discovery of pronounced mesoscopic effects such as Coulomb blockade and conductance quantization prompted the study of thermopower in quantum point contacts (Molenkamp *et al.*, 1990; van Houten *et al.*, 1992b; Molenkamp *et al.*, 1994) and quantum dots (Staring *et al.*, 1993; Godijn *et al.*, 1999; Scheibner *et al.*, 2005). These devices are defined by depositing gates on top of a two-dimensional electron gas formed in a semiconductor interface (typically GaAs/AlGaAs). Heating of one side of the device is achieved by passing current through it with consequent Joule heating and temperature rise. Most of the results of these experiments are well understood within the simple, single-particle picture of thermopower (van Houten *et al.*, 1992b), which will be described below.

Another, more recent batch of thermopower experiments are those conducted on nanowires, namely, wires with nanoscale diameter, but extending in the longitudinal direction as long as a few microns. Various experiments were performed on wires of different materials (Boukai *et al.*, 2006, 2007; Hochbaum *et al.*, 2007; Seol *et al.*, 2007; Duarte *et al.*, 2009; Lee *et al.*, 2009), as well as carbon nanotubes (Small *et al.*, 2003; Sumanasekera *et al.*, 2002; Kong *et al.*, 2005). These experiments suggest that in these systems it is possible to either increase S (by designing the system to have an increased electronic density of states) or reduce the thermal conductance independently by, e.g., designing a system which is smaller than the phonon mean-free path but still larger than the corresponding mean-free path of the electrons or holes, thus increasing the figure of merit. Specifically, in Si nanowires these are obtained by the combined effect of the change in phonon spectra and enhanced scattering off the boundary, both having little effect on the electronic part [see Rurali (2010)]. Along similar lines, boundary effects seem to highly reduce the thermal conductance but leave the charge conductance roughly unchanged (Majumdar, 2004).

A set of experiments which is of interest from both an academic and a technological point of view are those performed on junctions of nanometer length, such as metallic contacts (Ludoph and Ruitenbeek, 1999) or molecular junctions (Reddy *et al.*, 2007; Baheti *et al.*, 2008; Malen *et al.*, 2009a, 2009b; Tan *et al.*, 2010). The latter ones are of interest since, as we will discuss in Sec. IV.C, theoretical arguments suggest that molecular junctions may exhibit large thermopower. In these latter experiments, a gold STM tip is placed on top of a gold substrate which is covered with various molecules. As the STM tip touches (and is attached to) a molecule, a thermal gradient is applied and the thermopower is measured by applying a voltage so that no current passes through the junction (see upper panel of Fig. 9). This procedure is repeated many times and a histogram of the voltage required to achieve vanishing current is obtained [for different temperature gradients, $\Delta T = 10$, 20, and 30 K, Figs. 9(a)–9(c)]. They then plotted the voltage with maximum probability (i.e., the position of the peak in the voltage histograms) as a function of ΔT, and by fitting the resulting curve with a linear fit the thermopower is obtained [Fig. 9(d)]. These experiments were performed with various kinds of

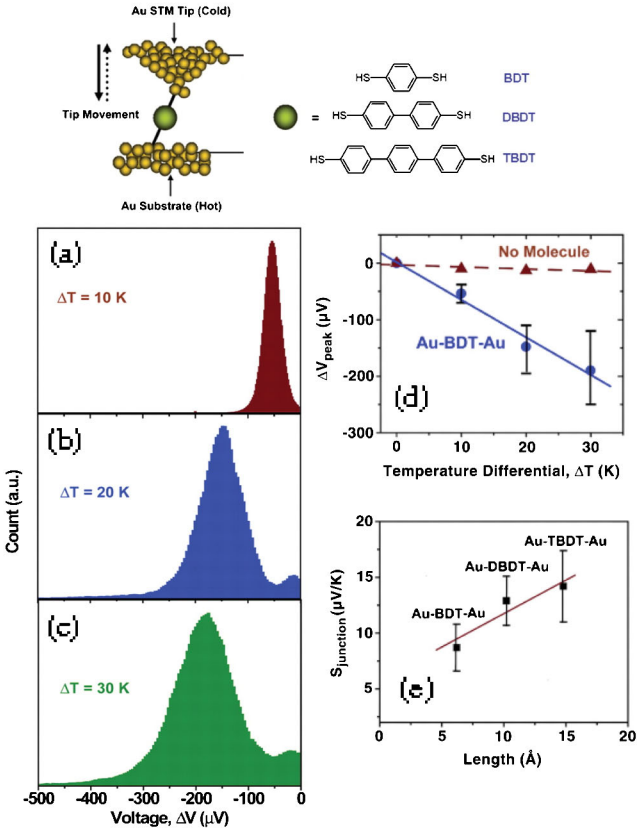

FIG. 9 (color online). Upper panel: Schematic representation of thermopower experiments on molecular junctions. (a)–(c) Distribution of thermovoltages obtained at different temperature gradients. Note the widening of the distributions and their nontrivial structure. (d) The most-probable thermovoltage obtained from (a)–(c) as a function of the temperature gradient. The derivative of the linear fit of this curve yields the thermopower S. (e) S of various molecules, in terms of the molecule's length. Adapted from Reddy *et al.*, 2007.

molecules, and interesting phenomena such as a length dependence of the thermopower [Fig. 9(e)] or strong dependence on the molecular end groups were observed. The experiments indicated that indeed molecular junctions have favorable thermoelectric properties, suggesting that devices incorporating molecular junctions or arrays (for instance, metallic plates separated by a molecular layer) may be good candidates for thermoelectric applications.

We, however, point out some features of the experiments which at present do not have a satisfactory theoretical explanation. For instance, as shown in Fig. 9(c), the voltage histograms have a well-defined structure, with a not-so-negligible secondary peak near $\Delta V = 0$. Note also that the distributions cross the $\Delta V = 0$ line into negative values, not shown in the figure. An additional feature of the histograms is their apparent widening with increasing temperature gradient. These fluctuation effects have been recently studied experimentally (Malen *et al.*, 2009a) and are attributed to variations in contact geometry and orbital hybridization, as well as intermolecular interactions, in accord with theoretical studies (Dubi and Di Ventra, 2009d).

Analysis of the above results has been done based on the single-particle (noninteracting) Landauer approach to thermopower. As discussed in Sec. IV.C, in the linear-response single-particle theory of thermopower, S can be simply related to the electronic properties of the junction, and specifically in molecular junctions, to the position of the electrochemical potentials of the leads with respect to the gap between the HOMO and the LUMO states. Since the position of the HOMO-LUMO gap affects charge transport in molecular junctions (Nitzan and Ratner, 2003), measurements of S were suggested as a way to probe the energy position of these levels (Paulsson and Datta, 2003; Baheti *et al.*, 2008). In the experiments (Reddy *et al.*, 2007; Baheti *et al.*, 2008), a comparison of the thermopower and conductance with numerical simulations using ground-state DFT within the Landauer approach was performed. From this comparison it was then concluded that the position of the HOMO-LUMO gap can be thus determined. This analysis, however, raises several questions. The applicability of a linear-response single-particle theory was questioned (Reddy *et al.*, 2007), following the fact that the temperature differences can be tens of degrees kelvin. In fact, one could ask if this is the smallest energy scale in the experiment. Specifically, is this energy smaller than, say, the coupling energy between the molecule and the substrate? The answer to this question is unclear, especially in light of the large error bars shown in Fig. 9(d). In addition, the nontrivial structure of the fluctuations in the voltage histogram implies that nonequilibrium effects may come into play, which are not taken into account in the linear-response theory. Finally, electron-electron and electron-phonon interactions may play a crucial role in this problem.

Despite these open questions, the experiments described above are impressive and important for the field and there are many interesting future directions to which they could be taken. For example, it would be interesting to study the change in the width of the distributions and their structures as the overall temperature is reduced. This would determine, e.g., if these distributions are due to static or dynamic effects. Another interesting direction would be to study, for several molecular structures, not just the most-probable voltage, but the real (statistical) average of the distributions, and infer from this whether the resulting thermopower displays the same features as reported above (e.g., length dependence, etc.), and whether this quantity matches calculations based on single-particle theories.

C. Theoretical methods

In this section we describe the present theoretical methods available to describe the phenomenon of thermopower. The most common one is based on the Landauer approach with its implementation within ground-state DFT. As we will discuss, this approach has several advantages, being rather computationally straightforward and having a rather simple physical interpretation. However, we argue that in many cases of actual experimental interest, it may be inadequate, since it is based on the usual assumptions of scattering theory of noninteracting electrons. In addition, as emphasized also in Sec. II.C.1, the use of ground-state DFT is questionable in an intrinsically nonequilibrium problem as the one discussed here. We then introduce an approach based on the theory of open quantum systems, which is ideally suited for the present problem and can, in principle, account for interactions (beyond mean-field). The latter point has its most practical implementation in an extension of time-dependent DFT to open quantum systems (Di Ventra and D'Agosta, 2007; D'Agosta and Di Ventra, 2008b).

1. Single-particle theory of thermopower

The starting point for calculating the thermopower within a single-particle picture is the Landauer expression for the electrical current (Butcher, 1990),

$$I = \frac{e}{\pi\hbar}\int_{-\infty}^{\infty} d\epsilon \mathcal{T}(\epsilon)[f_L(\epsilon) - f_R(\epsilon)], \tag{20}$$

where $\mathcal{T}(\epsilon)$ is the transmission coefficient at energy ϵ and $f_{L,R}$ are the Fermi distributions of the left and right leads. In the limit of small bias and temperature gradient (i.e., $|\Delta T| \ll T$ and $|e\Delta V| \ll \mu$, where T is the background temperature and μ is the equilibrium chemical potential), the distribution functions are given by (Butcher, 1990) ($i = L, R$)

$$f(\epsilon, \mu_i, T_i) \simeq f(\epsilon, \mu, T) \pm \frac{df}{d\epsilon}(\mu - \mu_i) \mp \frac{df}{d\epsilon}(\epsilon - \mu)\frac{(T_i - T)}{T}, \tag{21}$$

where now $f(\epsilon)$ is the equilibrium distribution and the $+$ and $-$ signs correspond to which electrochemical potential is higher or lower in energy with respect to the equilibrium chemical potential. Inserting this into Eq. (20) and equating the current to zero, one obtains

$$S(T) = \frac{1}{eT}\frac{\int_{-\infty}^{\infty} d\epsilon \mathcal{T}(\epsilon)(\epsilon - \mu)[-f'(\epsilon)]}{\int_{-\infty}^{\infty} d\epsilon \mathcal{T}(\epsilon)[-f'(\epsilon)]}. \tag{22}$$

Already from this result several features may be seen. First, since at $T = 0$ we have $-f'(\epsilon) = \delta(\epsilon - \mu)$, the numerator of S vanishes and $S(T = 0) = 0$. Second, even at finite temperatures $f'(\epsilon)$ is symmetric around μ, and therefore $S = 0$ unless

$\mathcal{T}(\epsilon)$ is not symmetric around μ. This is similar to the condition in bulk materials that requires the particle-hole symmetry be broken to have a finite thermopower (Ashcroft and Mermin, 1976).

One can further simplify $S(T)$ by taking the low-temperature limit and by assuming that there are no electronic resonances close to the equilibrium chemical potential. Using the Sommerfeld expansion to first order around $\mu(T=0)=\epsilon_F$ (Ashcroft and Mermin, 1976), one has

$$\int_{-\infty}^{\infty}\mathcal{T}(\epsilon)(\epsilon-\mu)f'(\epsilon)\approx\frac{\pi^2}{6}k_B^2T^2\frac{d^2[\mathcal{T}(\epsilon)(\epsilon-\mu)]}{d\epsilon^2}\bigg|_{\epsilon_F}=\frac{\pi^2}{3}k_B^2T^2\mathcal{T}'(\epsilon) \tag{23}$$

(where the second derivative comes from integration by parts) and one arrives at the expression for the thermopower,

$$S=\frac{\pi^2}{3}\frac{k_B}{e}k_BT\frac{d\ln[\mathcal{T}(\epsilon)]}{d\epsilon}\bigg|_{\epsilon_F}, \tag{24}$$

which is similar to Mott's semiclassical formula for bulk metals (Ashcroft and Mermin, 1976; Lunde and Flensberg, 2005). We stress again that this approximation is only valid at low temperatures and away from transmission resonances, so that the variation in $\mathcal{T}(\epsilon)$ is small.

The advantages of using the Landauer formalism are evident: It provides both a simple interpretation of the thermopower in terms of single-particle properties such as the transmission coefficient $\mathcal{T}(\epsilon)$ and a rather straightforward computational procedure. In fact, one needs only to determine the transmission coefficient $\mathcal{T}(\epsilon)$, which can be done as discussed in Sec. II.C.1. These reasons have made this approach extremely popular and widely used. An early use of Eq. (24) is in the study of thermopower in quantum point contacts (Molenkamp *et al.*, 1990; van Houten *et al.*, 1992b; Molenkamp *et al.*, 1994) and quantum dots (Staring *et al.*, 1993). In these mesoscopic systems, a gate voltage is used to tune either the width of the quantum point contacts or the energy levels in the quantum dots, giving rise to quantized conductance and Coulomb blockade. It turns out that in the cases above, the Landauer approach yields reasonably good agreement between theory and experiment (Molenkamp *et al.*, 1990), and knowledge of $\mathcal{T}(\epsilon)$ reasonably describes both the conductance and the thermopower. This would naively suggest that, for these types of systems, the above single-particle picture accounts for most of the thermopower. However, more recent investigations, which include effects of interactions, show that in both types of systems interactions may induce deviations from the Wiedmann-Franz law, thus reducing the agreement with experiments (Turek and Matveev, 2002; Turek *et al.*, 2005; Lunde *et al.*, 2006; Zhang, 2007; Kubala *et al.*, 2008), suggesting that the agreement in the single-particle case may be the result of the cancellation of errors.

In fact, despite its simplicity, the above approach suffers several shortcomings of particular relevance in nanoscale systems. The most prominent is the fact that it is formulated for noninteracting electrons. This means that any inclusion of interaction effects directly into $\mathcal{T}(\epsilon)$ can only be done at the mean-field level (Vignale and Di Ventra, 2009). To correct this, one should abandon the Landauer formula for the current, and, alternatively, use expressions for the currents obtained by using, e.g., the NEGF (Meir and Wingreen, 1992) or rate equations (Koch *et al.*, 2004). To our knowledge, in its fully interacting form NEGF was never employed to study the effects of electron interactions on the thermopower of molecular junctions.

Another limitation of the Landauer approach is the erroneous result it supplies in the zero-coupling limit. To demonstrate this, consider the simplest model for a nanoscale junction: a single resonant level symmetrically coupled to leads with spinless electrons (adding spin simply introduces a factor of 2). The transmission is given by a Breit-Wigner formula, $\mathcal{T}(\epsilon)=\Gamma^2/[\Gamma^2+(\epsilon-\epsilon_F)^2]$, where Γ is the lead-induced level broadening. Substituting into the expression for S [Eq. (24)] and taking the limit of $\Gamma\to 0$ gives a finite value, $S=-(2\pi^2/3)(k_B^2/e)[T/(\epsilon-\epsilon_F)]$. However, if one would consider a real device, it is clear that by detaching the leads would result in no temperature-induced voltage drop. The reason for this discrepancy is simple: In the linear-response calculation one assumes that the temperature difference is the smallest energy scale, yet in the limit $\Gamma\to 0$, Γ becomes comparable to such a scale, and the approximation breaks down. One should thus be careful both in using perturbation theory in the coupling between the leads and, say, a molecule in the junction and in comparing such calculations to experiments (see Sec. IV.C.2).

Much of the recent theoretical work on thermopower has been devoted to molecular junctions. Before we review some recent results, it is important to understand the origin of the specific interest in such systems, which may be understood from analyzing the Landauer formula (24). In a molecular junction, the Fermi energy of the leads is placed somewhere between the HOMO and LUMO states (i.e., in the HOMO-LUMO gap) (Nitzan and Ratner, 2003). The question is where exactly? The answer to this question cannot be answered by studying the conductance (or transmission) alone, which can be demonstrated through a simple example (Paulsson and Datta, 2003). Consider such a molecular junction, with HOMO and LUMO energies ϵ_{HOMO} and ϵ_{LUMO}, respectively. The transmission function can be modeled by a double Lorenzian, corresponding to tunneling via each of these levels independently, and assumes the following form:

$$\mathcal{T}(\epsilon)=\frac{\Gamma_L\Gamma_R}{\tilde{\Gamma}^2+(\epsilon_F-\epsilon_{\mathrm{HOMO}})^2}+\frac{\Gamma_L\Gamma_R}{\tilde{\Gamma}^2+(\epsilon_F-\epsilon_{\mathrm{LUMO}})^2}, \tag{25}$$

where $\Gamma_{L,R}$ is the level broadening due to the left (right) lead and $\tilde{\Gamma}=(\Gamma_L+\Gamma_R)/2$. (For simplicity, we assume it to be the same for the two levels.) The resulting thermopower [in units of $(\pi^2/3)(k_B^2/e)T$], along with the transmission coefficient, is plotted in Fig. 10 [taking $\tilde{\Gamma}/(\epsilon_{\mathrm{LUMO}}-\epsilon_{\mathrm{HOMO}})=0.1$]. As seen, according to this simple model, for a given value of transmission between ϵ_{LUMO} and ϵ_{HOMO}, there are two values of the Fermi energy which provide a solution to Eq. (25), and hence conductance alone does not suffice to determine the position of the Fermi energy. From the same model, however, one would infer that the sign of the thermopower is

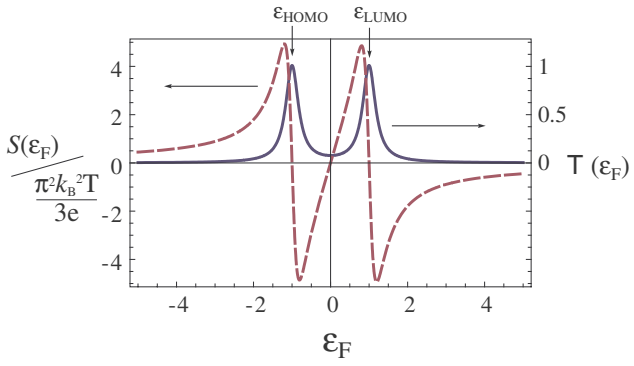

FIG. 10 (color online). Transmission (solid line) and normalized thermopower (dashed line) as a function of the position of the Fermi energy with respect to the HOMO-LUMO gap, based on the Landauer formula, Eq. (24), with approximation Eq. (25).

determined by the position of the Fermi energy from the center of the HOMO-LUMO gap, similar to the fact that the sign of the thermopower in bulk materials is determined by whether the conductance is dominated by electrons or holes (Ashcroft and Mermin, 1976), and therefore the sign of thermopower distinguishes between the two Fermi energies which solve Eq. (25).

This idea, along with the prospect of using molecular junctions as efficient thermoelectric devices, has generated much theoretical interest. To give a few examples, Segal (2005) showed that by measuring the thermopower one can distinguish between different electron transport mechanisms. Thermal and vibrational effects were studied in detail (Koch *et al.*, 2004) using rate equations, and it was shown that at low temperatures the signature of the vibrational modes on the thermopower can be measured. Murphy and Moore (2007) used rate equations to study the optimization of the figure of merit of a molecular junction, similar to the optimization of the figure of merit in bulk thermoelectrics (Mahan and Sofo, 1996).

Much recent attention has been devoted to studying the thermopower of molecular junctions using ground-state DFT to calculate $\mathcal{T}(\epsilon)$ combined with the Landauer formula (22) [or its even more simplified version Eq. (24)] (Paulsson and Datta, 2003; Zheng *et al.*, 2004; Wang *et al.*, 2005; Müller, 2008; Pauly *et al.*, 2008; Finch *et al.*, 2009; Ke *et al.*, 2009; Liu and Chen, 2009; Liu *et al.*, 2009b). In some cases, an impressive agreement has also been reported between the theoretical results and experiments (Ke *et al.*, 2009).

However, caution has to be applied in making such claims. In fact, if the system is away from linear response—and many experiments so far likely correspond to such a case—given a temperature difference, setting $I = 0$ in Eq. (20) does not necessarily provide a unique solution for the potential difference. In other words, there may be more than one potential difference ΔV that gives rise to the same ΔT (and hence several values of thermopower for the same temperature difference), when $I = 0$, as permitted by the nonlinearity of Eq. (20). In addition, as emphasized previously, even if the single-particle equations (22) and (24) were good starting points to describe the problem at hand, ground-state DFT is fundamentally flawed in the present context (even if one knew the exact ground-state functional) due to the fundamental nonequilibrium nature of the problem (Di Ventra and Todorov, 2004; Bushong *et al.*, 2005; Di Ventra, 2008; Vignale and Di Ventra, 2009). In this respect, even the interpretation of ground-state Kohn-Sham orbitals is questionable, since the latter ones are auxiliary quantities whose only role is to provide the correct density of the corresponding many-body system in its ground state.

To these limitations we must also add a few more physical issues. When a thermal gradient is applied to a junction, the transient dynamics is fundamental in establishing the voltage difference that enters the definition of thermopower. Since the dynamical formation of local resistivity dipoles creates strong local fields at the junction (especially at the nanoscale), these fields influence the electron motion in a nontrivial way and thus influence the long-time behavior of the carrier dynamics, even in the dc limit. This is particularly important *away* from the linear response (Di Ventra, 2008), which may be the experimental case.

It is the self-consistent formation of these fields that makes the thermopower very sensitive (both in magnitude and in sign) to atomic details and thus to the contact geometry between the nanostructure and bulk electrodes, as demonstrated also experimentally (Ludoph and Ruitenbeek, 1999). This precludes an easy interpretation in terms of ''electron'' or ''hole'' excitations as in bulk metals, and thus an easy relation with single-particle states (such as the HOMO and LUMO) as the Landauer equation (22) would imply. All this points to the fact that, since the system is in dynamical interaction with two different baths, one needs to go beyond the approximations underlying Eq. (22) and consider an open quantum system approach.

2. An open quantum system approach

We have precisely explored the problem of thermopower within the theory of open quantum systems (Dubi and Di Ventra, 2009d). In analogy with the idea that electrical currents may be studied using finite systems (Di Ventra and Todorov, 2004; Bushong *et al.*, 2005), one can study a finite system in contact with two heat baths held at different temperatures (i.e., finite leads connected by a nanoscale constriction, either a molecule, wire, etc.). If the system has a finite thermoelectric response then charges would flow between the leads until the ensuing electric potential ''balances'' the thermal gradient, and a charge imbalance is created between the two leads (which is related to the thermovoltage via the Poisson equation). Note that in this approach the system is allowed to find its own charge distribution via the transient dynamics (unlike a static approach where a static distribution is imposed *a priori* via boundary conditions), and even when the charge current is zero an *energy current* is still present, as in the actual experiments. Then, by calculating the thermally induced charge imbalance one obtains information on the thermoelectric response of the junction via the usual definitions. This approach is also not limited to linear response thus providing information on the thermovoltage even when the temperature gradient is not the smallest energy scale.

An implementation of such an open system approach can also be formulated within time-dependent DFT, thus allowing

one to include, in principle, all possible dynamical many-body effects in the thermopower (recall, in fact, that given the baths that set the temperature differences, the ensuing electrostatic voltage is a well-defined functional of the density). Indeed, Di Ventra and D'Agosta recently proved that if the bath-electron interactions are treated within a memoryless approximation (the thermal baths being Ohmic) (Van Kampen, 2001), then there is a one-to-one correspondence between the exact ensemble-averaged current density and the external vector potential, therefore extending the theorem (and Kohn-Sham scheme) of time-dependent current-DFT (TDCDFT) to open quantum systems (Di Ventra and D'Agosta, 2007; D'Agosta and Di Ventra, 2008b). The framework for this theory (named stochastic TDCDFT) is the stochastic Schrödinger equation, which describes a Hamiltonian quantum system in the presence of a bath (the extension to several baths is trivial) (Breuer and Petruccione, 2002) ($\hbar = 1$),

$$\dot{\Psi}(t) = -i\mathcal{H}\Psi(t) - \tfrac{1}{2}\hat{V}^{\dagger}\hat{V}\Psi(t) + l(t)\hat{V}\Psi(t). \tag{26}$$

Here $\Psi(t)$ is the many-body state vector, $\mathcal{H}$ is the Hamiltonian of the system (describing both the molecule and the leads and the coupling between them), $\hat{V}$ are the so-called bath operators (which could in principle be position and/or time dependent) (Van Kampen, 2001), which describe transitions between the different many-body states induced by the bath(s), and $l(t)$ is a stochastic field which is taken to have zero mean and a δ-function autocorrelation, $\langle l(t)\rangle = 0$, $\langle l(t)l(t')\rangle = \delta(t - t')$.

As a first demonstration, we used the method to study the thermopower of a simple model system of spinless noninteracting electrons, for which the calculations can be equivalently carried out with the density matrix rather than the state vector, by averaging over the stochastic realizations (Pershin *et al.*, 2008). In that model two planar leads, each in contact with a thermal bath at a given temperature, are connected via a nanoscale wire (see upper panel of Fig. 11). The bath-electron interactions are described by the operators

$$\hat{V}^{L,R}_{kk'} = \sqrt{\gamma^{L,R}_{kk'} f^{L,R}(\epsilon_k)}|k\rangle\langle k'|, \tag{27}$$

where $|k\rangle$ are the single-particle states of the Hamiltonian, $f^{L,R}$ is the Fermi function containing information on the left (right) bath temperature, and $\gamma^{L,R}_{kk'}$, which are the (inelastic) transition rates between states k and k', depend on the bath location (i.e., left or right) (Dubi and Di Ventra, 2009d). The corresponding equations of motion are then solved to obtain the wave function and hence the electron density, potential, and also the heat currents (see also Sec. III) at steady state.

Several interesting features are revealed by this model. For instance, the thermovoltage obtained shows nonlinear characteristics, which imply that the linear regime may not be the best regime to operate a thermoelectric device (Dubi and Di Ventra, 2009d). Another interesting feature is the strong dependence of the charge imbalance in the leads (and hence the thermopower) on the coupling between the wire (or molecule) and the leads. This confirms the experimental findings in metallic quantum point contacts (Ludoph and Ruitenbeek, 1999). In Fig. 11(a) (Dubi and Di Ventra, 2009d) the charge imbalance between the leads is plotted as a function of the ratio between the coupling between the wire and the left and right leads. From the figure it is obvious that the charge imbalance strongly fluctuates and can even change sign as a function of the wire-lead coupling. To demonstrate the importance of these fluctuations and to tie in with the experimental results presented in Sec. IV.B, we have performed a calculation for the same system as discussed by Dubi and Di Ventra (2009d), where the coupling constants were drawn from a normal distribution around typical values of $g = 0.1t$, where g is the lead-wire coupling and t is the tight-binding hopping parameter, which describes the bandwidth of the leads. Other numerical parameters are the filling fraction of electrons, $n = 1/3$, and the temperatures of the left and right heat baths, $T_L = 0.1$ and $T_R = 1$ (in units of t). A histogram of the resulting charge imbalance is plotted in Fig. 11(b), for three values of the width of the normal distribution, $\Delta g = 0.001$, 0.01, and 0.1 (in units of the hopping parameter). While more work needs to be done to explain the experimental data presented in Fig. 9(c), these theoretical results clearly bear some resemblance to experiments by showing a double structure in the charge imbalance as a function of the coupling asymmetry.

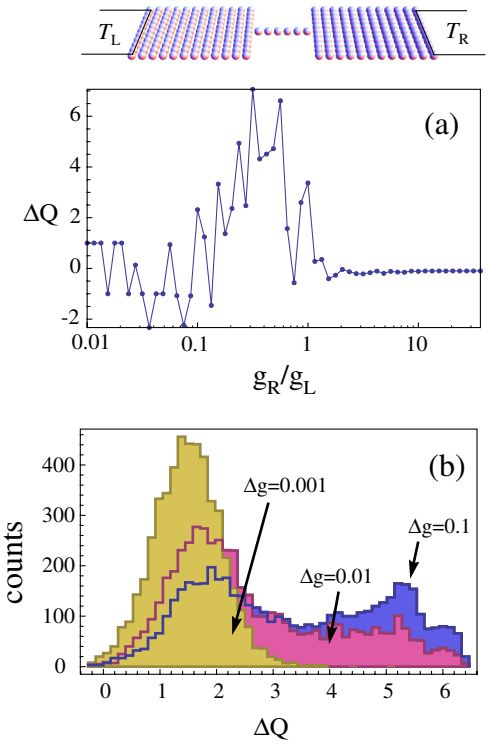

FIG. 11 (color online). Upper panel: Schematic representation of the model molecular junction composed of two quasi-two-dimensional leads connected with a molecular wire. The leads are coupled to external heat baths, each at its own temperature. (a) Electron charge imbalance as a function of the ratio between the couplings $g_{R(L)}$ between the wire and the right (left) lead. A strong dependence can be observed and even a change of sign. (b) Distribution of charge imbalance, when the couplings between the wire and the leads are drawn from a Gaussian distribution, with an average $g = 0.1$ and width $\Delta g = 0.001$, 0.01, and 0.1 in units of the hopping parameter (see text). From Dubi and Di Ventra, 2009d.

Using stochastic TDCDFT one can extend the above model system to interacting systems, as well as to a multicomponent formulation (Appel and Di Ventra, 2009), whereby the Hamiltonian now contains the correlated motion of electrons and (possibly quantum) ions, with both components interacting with an external environment. Such studies would shed new light on the role of interactions and ion dynamics on thermopower and enable a study of local heating effects in nanoscale systems (see also Sec. III). No results are, however, available yet for these cases.

V. SUMMARY AND FUTURE PROSPECTS

In this review we have discussed energy transport in nanoscale systems, such as molecular junctions, suspended nanotubes, quantum point contacts, etc. Our aim was to put the three major issues of thermal transport, namely, thermal conductance, local temperature and heating, and thermoelectricity under a unified theme. We have critically examined both theoretical and experimental aspects of these topics. We have presented many theoretical methods based on the single-particle scattering approach, nonequilibrium Green's functions formalism, molecular dynamics, etc. From the experimental side we have reviewed state-of-the-art experiments and stressed the difficulty and open questions in analyzing such experiments.

A. Future prospects

We conclude this review by presenting three novel ideas related to energy transport in nanoscale systems. These ideas, which deviate somewhat from the usual path of thermoelectricity and heat transport, reflect in our opinion the richness and usefulness of studying energy flow in nanoscale systems, and we hope will stimulate both the experimental and theoretical communities.

Thermospintronics.—Thermospintronics (sometimes called spin caloritronics) refers to the manipulation of electron spins with thermal effects. Generating spin currents, that is the flow of electron spins, plays an eminent role in the field of spintronics, which is the spin analog of electronics [see, e.g., Žutić *et al.* (2004)]. However, manipulating spins in order to generate spin currents is quite difficult, and it is equally hard to generate a spin current without generating an accompanying charge current. In recent experiments (Uchida *et al.*, 2008, 2009) a spin analog to the Seebeck effect was used to generate a spin voltage, induced by a temperature difference along a ferromagnetic slab. Although this effect is rather small (compared to its charge counterpart, but larger than expected in view of spin-flip scattering) and inherently induces an electric voltage as well, it has been suggested that these shortcomings may be overcome by applying a temperature gradient to a molecular junction placed between ferromagnetic leads (Dubi and Di Ventra, 2009e), a setup which was recently studied further (Lü *et al.*, 2010; Wang *et al.*, 2010; Ying and Jin, 2010). In another work, a variety of thermoelectric effects in magnetic junctions was studied (Hatami *et al.*, 2007, 2009; Heikkilä *et al.*, 2010), with unusual features such as thermal spin-transfer torque, spin-polarized cooling, and spin-heat coupling effects.

Enhanced thermopower in DNA.—DNA, the basic building block of our genetic code, also shows a large potential in nanotechnology applications (Dekker and Ratner, 2001; Di Ventra *et al.*, 2004; Zwolak and Di Ventra, 2008). In a recent study it was shown (Maciá, 2005, 2007), using a model Hamiltonian for different DNA-like chains, that under certain conditions the Seebeck coefficient and figure of merit of a lead-DNA-lead junction can be quite high and can rise to hundreds of μV/K, to be compared with a few μV/K of other single-molecule junctions studied so far. These high values of the thermopower seem to stem from transport resonance effects, which can be tuned rather easily in DNA. This, with the fact that there is a lot of know-how regarding DNA manipulation and preparation, makes DNA-based systems interesting candidates for future thermoelectric and cooling devices at the nanoscale.

Thermoelectricity in superconducting wires.—Raising the critical temperature T_c of superconducting materials is clearly a technologically important goal. However, most superconducting materials have a T_c well below room temperature, even in the well-known high-T_c materials (with $T_c \sim 80$ K for wires and $T_c \sim 200$ K for bulk). Recently, we suggested (Dubi and Di Ventra, 2009a) studying a superconducting wire held at two different temperatures at its edges. Using the method introduced in Sec. IV.C.2 combined with a self-consistent mean-field theory, it was shown that for an (ideally) clean superconducting wire, if one of the sides (the cold side) is held at low enough temperatures, the temperature of the hot side can be much larger than the equilibrium T_c, with the wire still in its superconducting state. Although this study neglects some effects (such as phase fluctuations), the basic idea is simple: In order to have a superconducting wire, instead of cooling down the entire apparatus, one can *locally* cool the wire by attaching to it a local refrigerator, e.g., one made from a Peltier cooling device (Shakouri, 2006). This may pave the road for hybrid superconducting circuits which operate at relatively high temperatures.

B. Final thoughts

These last few examples—and what we have discussed in this Colloquium—show that the quest to understand energy transport in nanostructures is far from over. In fact, it seems to us that we have barely scratched the surface of this problem and more discoveries await us. Regarding thermal conductance, finding systems that show either very good (for nanoelectronic applications) or very poor (for thermoelectric applications) thermal conductance is needed. As for thermoelectricity, there is a need to advance our theoretical tools quite substantially. For instance, theories that account for the statistical nature of the experiments should be developed that include also electron-electron and electron-phonon interactions on equal footing. In addition, since the problem is intrinsically out of equilibrium (even at steady state), these theories need to include dynamical effects. As for local heating and local temperatures, the handful of experiments that have appeared recently are certainly a good start, but more are needed in order to truly determine the processes leading to heating (and cooling) in nanoscale junctions. Similarly,

more experiments that could directly determine the validity (or invalidity) of Fourier's law are highly desirable.

Because of the rapid developments in science and technology it is difficult to predict where the field will go from here. However, there is no doubt that novel and ingenious ideas will be put forth that will help us profit from energy flow, storage, and conversion. Embarking on such a quest could not be more timely.

ACKNOWLEDGMENTS

We thank D. Roy for useful discussions and a critical reading of the manuscript. This work has been supported by the DOE under Grant No. DE-FG02-05ER46204 and the University of California Laboratories.

REFERENCES

Akkermans, E., and G. Montambaux, 2007, *Mesoscopic Physics of Electrons and Photons* (Cambridge University Press, Cambridge, England).
Ando, T., 1991, Phys. Rev. B **44**, 8017.
Angelescu, D. E., M. C. Cross, and M. L. Roukes, 1998, Superlattices Microstruct. **23**, 673.
Appel, H., and M. Di Ventra, 2009, Phys. Rev. B **80**, 212303.
Appleyard, N. J., J. T. Nicholls, M. Pepper, W. R. Tribe, M. Y. Simmons, and D. A. Ritchie, 2000, Phys. Rev. B **62**, R16275.
Ashcroft, N. W., and N. D. Mermin, 1976, *Solid State Physics* (Brooks-Cole, Belmont, MA).
Baheti, K., J. A. Malen, P. Doak, P. Reddy, S.-Y. Jang, T. D. Tilley, A. Majumdar, and R. A. Segalman, 2008, Nano Lett. **8**, 715.
Balandin, A. A., S. Ghosh, W. Bao, I. Calizo, D. Teweldebrhan, F. Miao, and C. N. Lau, 2008, Nano Lett. **8**, 902.
Bell, L. E., 2008, Science **321**, 1457.
Berber, S., Y.-K. Kwon, and D. Tománek, 2000, Phys. Rev. Lett. **84**, 4613.
Blencowe, M., 1999, Phys. Rev. B **59**, 4992.
Blencowe, M., 2004, Phys. Rep. **395**, 159.
Bonetto, F., J. Lebowitz, and J. Lukkarinen, 2004, J. Stat. Phys. **116**, 783.
Bonetto, F., J. L. Lebowitz, and L. Rey-Bellet, 2000, in *Mathematical Physics 2000*, edited by A. Fokas, A. Grigoryan, T. Kibble, and B. Zegarlinski (Imperial College Press, London, UK), p. 128.
Boukai, A., K. Xu, and J. Heath, 2006, Adv. Mater. **18**, 864.
Boukai, A. I., Y. Bunimovich, J. Tahir-Kheli, J.-K. Yu, W. A. Goddard, III, and J. R. Heath, 2008, Nature (London) **451**, 168.
Bourgeois, O., T. Fournier, and J. Chaussy, 2007, J. Appl. Phys. **101**, 016104.
Breuer, H. P., and F. Petruccione, 2002, *Theory of Open Quantum Systems* (Oxford University Press, New York).
Brown, E., L. Hao, J. C. Gallop, and J. C. Macfarlane, 2005, Appl. Phys. Lett. **87**, 023107.
Bushmaker, A. W., V. V. Deshpande, M. W. Bockrath, and S. B. Cronin, 2007, Nano Lett. **7**, 3618.
Bushong, N., N. Sai, and M. Di Ventra, 2005, Nano Lett. **5**, 2569.
Butcher, P., 1990, J. Phys. Condens. Matter **2**, 4869.
Büttiker, M., Y. Imry, R. Landauer, and S. Pinhas, 1985, Phys. Rev. B **31**, 6207.
Cahill, D. G., 1990, Rev. Sci. Instrum. **61**, 802.
Cahill, D. G., W. K. Ford, K. E. Goodson, G. D. Mahan, A. Majumdar, H. J. Maris, R. Merlin, and S. R. Phillpot, 2003, J. Appl. Phys. **93**, 793.
Calizo, I., A. A. Balandin, W. Bao, F. Miao, and C. N. Lau, 2007, Nano Lett. **7**, 2645.
Carruthers, P., 1961, Rev. Mod. Phys. **33**, 92.
Caso, A., L. Arrachea, and G. S. Lozano, 2010, Phys. Rev. B **81**, 041301.
Chalopin, Y., J.-N. Gillet, and S. Volz, 2008, Phys. Rev. B **77**, 233309.
Chang, C. W., A. M. Fennimore, A. Afanasiev, D. Okawa, T. Ikuno, H. Garcia, D. Li, A. Majumdar, and A. Zettl, 2006, Phys. Rev. Lett. **97**, 085901.
Chang, C. W., D. Okawa, H. Garcia, A. Majumdar, and A. Zettl, 2008, Phys. Rev. Lett. **101**, 075903.
Chen, G., 2005, *Nanoscale Energy Transport and Conversion* (Oxford University Press, New York).
Chen, R., A. I. Hochbaum, P. Murphy, J. Moore, P. Yang, and A. Majumdar, 2008, Phys. Rev. Lett. **101**, 105501.
Chen, K.-Q., W.-X. Li, W. Duan, Z. Shuai, and B.-L. Gu, 2005, Phys. Rev. B **72**, 045422.
Chen, Y.-C., 2008, Phys. Rev. B **78**, 233310.
Chen, Y.-C., M. Zwolak, and M. Di Ventra, 2003, Nano Lett. **3**, 1691.
Chen, Y.-C., M. Zwolak, and M. Di Ventra, 2005, Nano Lett. **5**, 621.
Cheng, C.-L., J. S. Evans, and T. Van Voorhis, 2006, Phys. Rev. B **74**, 155112.
Chiatti, O., J. T. Nicholls, Y. Y. Proskuryakov, N. Lumpkin, I. Farrer, and D. A. Ritchie, 2006, Phys. Rev. Lett. **97**, 056601.
Chiu, H.-Y., V. V. Deshpande, H. W. C. Postma, C. N. Lau, C. Mikó, L. Forró, and M. Bockrath, 2005, Phys. Rev. Lett. **95**, 226101.
Choi, T. Y., D. Poulikakos, J. Tharian, and U. Sennhauser, 2005, Appl. Phys. Lett. **87**, 013108.
Choi, T.-Y., D. Poulikakos, J. Tharian, and U. Sennhauser, 2006, Nano Lett. **6**, 1589.
D'Agosta, R., and M. Di Ventra, 2006, J. Phys. Condens. Matter **18**, 11059.
D'Agosta, R., and M. Di Ventra, 2008a, J. Phys. Condens. Matter **20**, 374102.
D'Agosta, R., and M. Di Ventra, 2008b, Phys. Rev. B **78**, 165105.
D'Agosta, R., N. Sai, and M. Di Ventra, 2006, Nano Lett. **6**, 2935.
Datta, S., 1997, *Electronic Transport in Mesoscopic Systems* (Cambridge University Press, Cambridge, England).
Dekker, C., and M. A. Ratner, 2001, Phys. World **14**, 29, http://physicsworld.com/cws/article/print/60.
Deshpande, V. V., S. Hsieh, A. W. Bushmaker, M. Bockrath, and S. B. Cronin, 2009, Phys. Rev. Lett. **102**, 105501.
Dhar, A., 2008, Adv. Phys. **57**, 457.
Dhar, A., and J. L. Lebowitz, 2008, Phys. Rev. Lett. **100**, 134301.
Dhar, A., and D. Roy, 2006, J. Stat. Phys. **125**, 801.
Di Ventra, M., 2008, *Electrical Transport in Nanoscale Systems* (Cambridge University Press, Cambridge, England).
Di Ventra, M., and R. D'Agosta, 2007, Phys. Rev. Lett. **98**, 226403.
Di Ventra, M., and Y. Dubi, 2009, Europhys. Lett. **85**, 40004.
Di Ventra, M., S. Evoy, J. E. James, and R. Heflin, 2004, *Introduction to Nanoscale Science and Technology* (Kluwer Academic Publishers, Dordrecht, The Netherlands).
Di Ventra, M., and N. Lang, 2001, Phys. Rev. B **65**, 045402.
Di Ventra, M., and T. N. Todorov, 2004, J. Phys. Condens. Matter **16**, 8025.
Duarte, N. B., G. D. Mahan, and S. Tadigadapa, 2009, Nano Lett. **9**, 617.
Dubi, Y., and M. Di Ventra, 2009a (unpublished).
Dubi, Y., and M. Di Ventra, 2009b, Phys. Rev. E **79**, 042101.
Dubi, Y., and M. Di Ventra, 2009c, Phys. Rev. B **79**, 115415.
Dubi, Y., and M. Di Ventra, 2009d, Nano Lett. **9**, 97.
Dubi, Y., and M. Di Ventra, 2009e, Phys. Rev. B **79**, 081302.

Esposito, M., K. Lindenberg, and C. V. den Broeck, 2009, Europhys. Lett. **85**, 60010.
Feldman, J. L., D. J. Singh, I. I. Mazin, D. Mandrus, and B. C. Sales, 2000, Phys. Rev. B **61**, R9209.
Fermi, E., J. Pasta, and S. Ulam, 1955, Los Alamos Report No. LA-1940.
Finch, C. M., V. M. García-Suárez, and C. J. Lambert, 2009, Phys. Rev. B **79**, 033405.
Fourier, J., 1822, *Theorie Analytique de la Chaleur* (Didot, Paris).
Franceschi, S. D., and N. Mingo, 2007, Nature Nanotech. **2**, 537.
Fujii, M., X. Zhang, H. Xie, H. Ago, K. Takahashi, T. Ikuta, H. Abe, and T. Shimizu, 2005, Phys. Rev. Lett. **95**, 065502.
Galperin, M., A. Nitzan, and M. A. Ratner, 2007, Phys. Rev. B **75**, 155312.
Galperin, M., M. A. Ratner, and A. Nitzan, 2007, J. Phys. Condens. Matter **19**, 103201.
Galperin, M., M. A. Ratner, and A. Nitzan, 2009, Nano Lett. **9**, 758.
Galperin, M., K. Saito, A. V. Balatsky, and A. Nitzan, 2009, Phys. Rev. B **80**, 115427.
Garg, A., D. Rasch, E. Shimshoni, and A. Rosch, 2009, Phys. Rev. Lett. **103**, 096402.
Gaul, C., and H. Büttner, 2007, Phys. Rev. E **76**, 011111.
Giazotto, F., T. T. Heikkilä, A. Luukanen, A. M. Savin, and J. P. Pekola, 2006, Rev. Mod. Phys. **78**, 217.
Godijn, S. F., S. Möller, H. Buhmann, L. W. Molenkamp, and S. A. van Langen, 1999, Phys. Rev. Lett. **82**, 2927.
Greiner, A., L. Reggiani, T. Kuhn, and L. Varani, 1997, Phys. Rev. Lett. **78**, 1114.
Grover, R., B. McCarthy, D. Sarid, and I. Guven, 2006, Appl. Phys. Lett. **88**, 233501.
Hartmann, M., and G. Mahler, 2005, Europhys. Lett. **70**, 579.
Hartmann, M., G. Mahler, and O. Hess, 2004a, Phys. Rev. Lett. **93**, 080402.
Hartmann, M., G. Mahler, and O. Hess, 2004b, Phys. Rev. E **70**, 066148.
Hatami, M., G. E. W. Bauer, Q. Zhang, and P. J. Kelly, 2007, Phys. Rev. Lett. **99**, 066603.
Hatami, M., G. E. W. Bauer, Q. Zhang, and P. J. Kelly, 2009, Phys. Rev. B **79**, 174426.
Heikkilä, T. T., M. Hatami, and G. E. W. Bauer, 2010, Phys. Rev. B **81**, 100408.
Henry, A., and G. Chen, 2008, Phys. Rev. Lett. **101**, 235502.
Henry, A. S., and G. Chen, 2008, J. Comput. Theor. Nanosci. **5**, 141.
Hochbaum, A. I., R. Chen, R. D. Delgado, W. Liang, E. C. Garnett, M. Najarian, A. Majumdar, and P. Yang, 2008, Nature (London) **451**, 163.
Hoffmann, E. A., H. A. Nilsson, J. E. Matthews, N. Nakpathomkun, A. I. Persson, L. Samuelson, and H. Linke, 2009, Nano Lett. **9**, 779.
Hoover, W. G., 1985, Phys. Rev. A **31**, 1695.
Hsu, I.-K., M. T. Pettes, A. Bushmaker, M. Aykol, L. Shi, and S. B. Cronin, 2009, Nano Lett. **9**, 590.
Hu, M., P. Keblinski, J.-S. Wang, and N. Raravikar, 2008, J. Appl. Phys. **104**, 083503.
Huang, Z., F. Chen, R. D'Agosta, P. A. Bennett, M. Di Ventra, and N. Tao, 2007, Nature Nanotech. **2**, 698.
Huang, Z., B. Xu, Y. Chen, M. Di Ventra, and N. Tao, 2006, Nano Lett. **6**, 1240.
Imry, Y., 1997, *Introduction to Mesoscopic Physics* (Oxford University Press, New York).
Ioffe, Z., T. Shamai, A. Ophir, G. Noy, I. Yutsis, K. Kfir, O. Cheshnovsky, and Y. Selzer, 2008, Nature Nanotech. **3**, 727.
Jacquet, P., 2009, J. Stat. Phys. **134**, 709.
Kadanoff, L. P., and G. Baym, 1962, *Quantum Statistical Mechanics* (Benjamin, New York).
Kambili, A., G. Fagas, V. I. Fal'ko, and C. J. Lambert, 1999, Phys. Rev. B **60**, 15593.
Kane, C. L., and M. P. A. Fisher, 1996, Phys. Rev. Lett. **76**, 3192.
Ke, S.-H., W. Yang, S. Curtarolo, and H. U. Baranger, 2009, Nano Lett. **9**, 1011.
Keldysh, L. V., 1964, Zh. Eksp. Teor. Fiz. **47**, 1515 [Sov. Phys. JETP **20**, 1018 (1965)].
Khomyakov, P. A., and G. Brocks, 2004, Phys. Rev. B **70**, 195402.
Kim, K., J. Chung, J. Won, O. Kwon, J. S. Lee, S. H. Park, and Y. K. Choi, 2008, Appl. Phys. Lett. **93**, 203115.
Kim, P., L. Shi, A. Majumdar, and P. L. McEuen, 2001, Phys. Rev. Lett. **87**, 215502.
Koch, J., M. Semmelhack, F. von Oppen, and A. Nitzan, 2006, Phys. Rev. B **73**, 155306.
Koch, J., F. von Oppen, Y. Oreg, and E. Sela, 2004, Phys. Rev. B **70**, 195107.
Kong, W. J., L. Lu, H. W. Zhu, B. Q. Wei, and D. H. Wu, 2005, J. Phys. Condens. Matter **17**, 1923.
Kubala, B., J. König, and J. Pekola, 2008, Phys. Rev. Lett. **100**, 066801.
Kundu, A., A. Dhar, and O. Narayan, 2009, J. Stat. Mech., L03001.
Lan, J., J.-S. Wang, C. K. Gan, and S. K. Chin, 2009, Phys. Rev. B **79**, 115401.
Landauer, R., 1957, IBM J. Res. Dev. **1**, 223.
Landauer, R., 1970, Philos. Mag. **21**, 863.
Lee, C.-H., G.-C. Yi, Y. M. Zuev, and P. Kim, 2009, Appl. Phys. Lett. **94**, 022106.
Lepri, S., R. Livi, and A. Politi, 1997, Phys. Rev. Lett. **78**, 1896.
Lepri, S., R. Livi, and A. Politi, 2003, Phys. Rep. **377**, 1.
Li, B., L. Wang, and G. Casati, 2004, Phys. Rev. Lett. **93**, 184301.
Li, B., L. Wang, and G. Casati, 2006, Appl. Phys. Lett. **88**, 143501, http://link.aip.org/link/?APL/88/143501/1.
Li, B., L. Wang, and B. Hu, 2002, Phys. Rev. Lett. **88**, 223901.
Li, B. W., L. Wang, and G. Casati, 2004, Phys. Rev. Lett. **93**, 184301.
Li, D., Y. Wu, P. Kim, L. Shi, P. Yang, and A. Majumdar, 2003, Appl. Phys. Lett. **83**, 2934.
Li, M.-R., and E. Orignac, 2002, Europhys. Lett. **60**, 432.
Liu, H.-P., and L. Yi, 2006, Chin. Phys. Lett. **23**, 3194.
Liu, J., J. Song, Q.-F. Sun, and X. C. Xie, 2009, Phys. Rev. B **79**, 161309.
Liu, Y.-S., and Y.-C. Chen, 2009, Phys. Rev. B **79**, 193101.
Liu, Y.-S., Y.-R. Chen, and Y.-C. Chen, 2009b, ACS Nano **3**, 3497.
Lo, W. C., L. Wang, and B. Li, 2008, J. Phys. Soc. Jpn. **77**, 054402.
Lü, H.-F., L.-C. Zhu, X.-T. Zu, and H.-W. Zhang, 2010, Appl. Phys. Lett. **96**, 123111.
Lü, J. T., and J.-S. Wang, 2007, Phys. Rev. B **76**, 165418.
Lü, J. T., and J.-S. Wang, 2008, Phys. Rev. B **78**, 235436.
Lu, L., W. Yi, and D. L. Zhang, 2001, Rev. Sci. Instrum. **72**, 2996.
Ludoph, B., and J. M. v. Ruitenbeek, 1999, Phys. Rev. B **59**, 12290.
Lunde, A. M., and K. Flensberg, 2005, J. Phys. Condens. Matter **17**, 3879.
Lunde, A. M., K. Flensberg, and L. I. Glazman, 2006, Phys. Rev. Lett. **97**, 256802.
Luttinger, J. M., 1964, Phys. Rev. **135**, A1505.
Maciá, E., 2005, Nanotechnology **16**, S254.
Maciá, E., 2007, Phys. Rev. B **75**, 035130.
Mahan, G. D., and J. O. Sofo, 1996, Proc. Natl. Acad. Sci. U.S.A. **93**, 7436.
Majumdar, A., 2004, Science **303**, 777.

Malen, J. A., P. Doak, K. Baheti, T. D. Tilley, A. Majumdar, and R. A. Segalman, 2009a, Nano Lett. **9**, 3406.
Malen, J. A., P. Doak, K. Baheti, T. D. Tilley, R. A. Segalman, and A. Majumdar, 2009b, Nano Lett. **9**, 1164.
Maynard, R., and E. Akkermans, 1985, Phys. Rev. B **32**, 5440.
McEniry, E. J., T. N. Todorov, and D. Dundas, 2009, J. Phys. Condens. Matter **21**, 195304.
Meir, Y., and N. S. Wingreen, 1992, Phys. Rev. Lett. **68**, 2512.
Mejia-Monasterio, C., and H. Wichterich, 2007, Eur. Phys. J. Special Topics **151**, 113.
Meschke, M., W. Guichard, and J. P. Pekola, 2006, Nature (London) **444**, 187.
Michel, M., J. Gemmer, and G. Mahler, 2006, Int. J. Mod. Phys. B **20**, 4855.
Michel, M., M. Hartmann, J. Gemmer, and G. Mahler, 2003, Eur. Phys. J. B **34**, 325.
Mingo, N., 2006, Phys. Rev. B **74**, 125402.
Mingo, N., and D. A. Broido, 2005a, Phys. Rev. Lett. **95**, 096105.
Mingo, N., and D. A. Broido, 2005b, Nano Lett. **5**, 1221.
Mingo, N., and L. Yang, 2003, Phys. Rev. B **68**, 245406.
Mingo, N., L. Yang, D. Li, and A. Majumdar, 2003, Nano Lett. **3**, 1713.
Molenkamp, L., A. A. M. Staring, B. W. Alphenaar, H. van Houten, and C. W. J. Beenakker, 1994, Semicond. Sci. Technol. **9**, 903.
Molenkamp, L. W., H. van Houten, C. W. J. Beenakker, R. Eppenga, and C. T. Foxon, 1990, Phys. Rev. Lett. **65**, 1052.
Mozyrsky, D., M. B. Hastings, and I. Martin, 2006, Phys. Rev. B **73**, 035104.
Müller, K.-H., 2008, J. Chem. Phys. **129**, 044708.
Murphy, P., S. Mukerjee, and J. Moore, 2008, Phys. Rev. B **78**, 161406.
Murphy, P. G., and J. E. Moore, 2007, Phys. Rev. B **76**, 155313.
Nicholls, J. T., and O. Chiatti, 2008, J. Phys. Condens. Matter **20**, 164210.
Nitzan, A., and M. A. Ratner, 2003, Science **300**, 1384.
Nosé, S., 1984, J. Chem. Phys. **81**, 511.
Ozpineci, A., and S. Ciraci, 2001, Phys. Rev. B **63**, 125415.
Padgett, C. W., and D. W. Brenner, 2004, Nano Lett. **4**, 1051.
Padgett, C. W., O. Shenderova, and D. W. Brenner, 2006, Nano Lett. **6**, 1827.
Paulsson, M., and S. Datta, 2003, Phys. Rev. B **67**, 241403.
Pauly, F., J. K. Viljas, and J. C. Cuevas, 2008, Phys. Rev. B **78**, 035315.
Peierls, R., 1929, Ann. Phys. (Berlin) **395**, 1055.
Peierls, R. E., 1955, *Quantum Theory of Solids* (Oxford University Press, New York).
Pekola, J. P., T. T. Heikkilä, A. M. Savin, J. T. Flyktman, F. Giazotto, and F. W. J. Hekking, 2004, Phys. Rev. Lett. **92**, 056804.
Pendry, J. B., 1983, J. Phys. A **16**, 2161.
Peng, X.-F., K.-Q. Chen, B. S. Zou, and Y. Zhang, 2007, Appl. Phys. Lett. **90**, 193502.
Pershin, Y. V., Y. Dubi, and M. Di Ventra, 2008, Phys. Rev. B **78**, 054302.
Pistolesi, F., 2009, J. Low Temp. Phys. **154**, 199.
Ponomareva, I., D. Srivastava, and M. Menon, 2007, Nano Lett. **7**, 1155.
Pop, E., D. Mann, Q. Wang, K. Goodson, and H. Dai, 2006, Nano Lett. **6**, 96.
Reddy, P., S.-Y. Jang, R. A. Segalman, and A. Majumdar, 2007, Science **315**, 1568.
Rego, L. G. C., 2001, Phys. Status Solidi A **187**, 239.
Rego, L. G. C., and G. Kirczenow, 1998, Phys. Rev. Lett. **81**, 232.
Rejec, T., A. Ramšak, and J. H. Jefferson, 2002, Phys. Rev. B **65**, 235301.
Ren, S.-F., W. Cheng, and G. Chen, 2006, J. Appl. Phys. **100**, 103505.
Rodgers, P., 2008, Nature Nanotech. **3**, 76.
Roy, D., 2008, Phys. Rev. E **77**, 062102.
Roy, D., and A. Dhar, 2008, Phys. Rev. E **78**, 051112.
Runge, E., and E. K. U. Gross, 1984, Phys. Rev. Lett. **52**, 997.
Rurali, R., 2010, Rev. Mod. Phys. **82**, 427.
Saira, O.-P., M. Meschke, F. Giazotto, A. M. Savin, M. Möttönen, and J. P. Pekola, 2007, Phys. Rev. Lett. **99**, 027203.
Saito, K., 2003, Europhys. Lett. **61**, 34.
Santamore, D. H., and M. C. Cross, 2001, Phys. Rev. B **63**, 184306.
Savić, I., N. Mingo, and D. A. Stewart, 2008, Phys. Rev. Lett. **101**, 165502.
Savić, I., D. A. Stewart, and N. Mingo, 2008, Phys. Rev. B **78**, 235434.
Scheibner, R., H. Buhmann, D. Reuter, M. N. Kiselev, and L. W. Molenkamp, 2005, Phys. Rev. Lett. **95**, 176602.
Scheibner, R., E. G. Novik, T. Borzenko, M. König, D. Reuter, A. D. Wieck, H. Buhmann, and L. W. Molenkamp, 2007, Phys. Rev. B **75**, 041301.
Schmidt, D. R., R. J. Schoelkopf, and A. N. Cleland, 2004, Phys. Rev. Lett. **93**, 045901.
Schulze, G., *et al.*, 2008, Phys. Rev. Lett. **100**, 136801.
Schwab, K., E. Henriksen, J. Worlock, and M. Roukes, 2000, Nature (London) **404**, 974.
Segal, D., 2005, Phys. Rev. B **72**, 165426.
Segal, D., and A. Nitzan, 2005, Phys. Rev. Lett. **94**, 034301.
Segal, D., A. Nitzan, and P. Hänggi, 2003, J. Chem. Phys. **119**, 6840.
Seol, J. H., A. L. Moore, S. K. Saha, F. Zhou, L. Shi, Q. L. Ye, R. Scheffler, N. Mingo, and T. Yamada, 2007, J. Appl. Phys. **101**, 023706.
Shakouri, A., 2006, Proc. IEEE **94**, 1613.
Shi, L., D. Li, C. Yu, W. Jang, D. Kim, Z. Yao, P. Kim, and A. Majumdar, 2003, J. Heat Transfer **125**, 881.
Small, J. P., K. M. Perez, and P. Kim, 2003, Phys. Rev. Lett. **91**, 256801.
Staring, A. A. M., L. W. Molenkamp, B. W. Alphenaar, H. van Houten, O. J. A. Buyk, M. A. A. Mabesoone, C. W. J. Beenakker, and C. T. Foxon, 1993, Europhys. Lett. **22**, 57.
Stewart, D. A., I. Savić, and N. Mingo, 2009, Nano Lett. **9**, 81.
Sumanasekera, G. U., B. K. Pradhan, H. E. Romero, K. W. Adu, and P. C. Eklund, 2002, Phys. Rev. Lett. **89**, 166801.
Tan, A., S. Sadat, and P. Reddy, 2010, Appl. Phys. Lett. **96**, 013110.
Tanaka, Y., F. Yoshida, and S. Tamura, 2005, Phys. Rev. B **71**, 205308.
Tang, L.-M., L.-L. Wang, K.-Q. Chen, W.-Q. Huang, and B. S. Zou, 2006, Appl. Phys. Lett. **88**, 163505.
Tang, L.-M., L. Wang, W.-Q. Huang, B. S. Zou, and K.-Q. Chen, 2007, J. Phys. D **40**, 1497.
Teramae, Y., K. Horiguchi, S. Hashimoto, M. Tsutsui, S. Kurokawa, and A. Sakai, 2008, Appl. Phys. Lett. **93**, 083121.
Terraneo, M., M. Peyrard, and G. Casati, 2002, Phys. Rev. Lett. **88**, 094302.
Ting, D. Z. Y., E. T. Yu, and T. C. McGill, 1992, Phys. Rev. B **45**, 3583.
Todorov, T., 1998, Philos. Mag. B **77**, 965.
Tong, P., B. Li, and B. Hu, 1999, Phys. Rev. B **59**, 8639.
Tsutsui, M., S. Kurokawa, and A. Sakai, 2007, Appl. Phys. Lett. **90**, 133121.

Tsutsui, M., K. Shoji, K. Morimoto, M. Taniguchi, and T. Kawai, 2008, Appl. Phys. Lett. **92**, 223110.
Tsutsui, M., M. Taniguchi, and T. Kawai, 2008, Nano Lett. **8**, 3293.
Turek, M., and K. A. Matveev, 2002, Phys. Rev. B **65**, 115332.
Turek, M., J. Siewert, and K. Richter, 2005, Phys. Rev. B **71**, 220503.
Turney, J. E., E. S. Landry, A. J. H. McGaughey, and C. H. Amon, 2009, Phys. Rev. B **79**, 064301.
Uchida, K., S. Takahashi, K. Harii, J. Ieda, W. Koshibae, K. Ando, S. Maekawa, and E. Saitoh, 2008, Nature (London) **455**, 778.
Uchida, K., S. Takahashi, J. Ieda, K. Harii, K. Ikeda, W. Koshibae, S. Maekawa, and E. Saitoh, 2009, J. Appl. Phys. **105**, 07C908.
USDOE, 2009, Advanced Thermoelectric Materials for Efficient Waste Heat Recovery in Process Industries, http://www1.eere.energy.gov/.
van Houten, H., L. W. Molenkamp, C. W. J. Beenakker, and C. T. Foxon, 1992a, Semicond. Sci. Technol. **7**, B215.
van Houten, H., L. W. Molenkamp, C. W. J. Beenakker, and C. T. Foxon, 1992b, Semicond. Sci. Technol. **7**, B215.
Van Kampen, N. G., 2001, *Stochastic Processes in Physics and Chemistry* (North-Holland, Amsterdam).
van Wees, B. J., H. van Houten, C. W. J. Beenakker, J. G. Williamson, L. P. Kouwenhoven, D. van der Marel, and C. T. Foxon, 1988, Phys. Rev. Lett. **60**, 848.
Vignale, G., and M. Di Ventra, 2009, Phys. Rev. B **79**, 014201.
Volz, S., 2009, Ed., *Thermal Nanosystems and Nanomaterials*, Topics in Applied Physics (Springer, New York).
Wang, B., Y. Xing, L. Wan, Y. Wei, and J. Wang, 2005, Phys. Rev. B **71**, 233406.
Wang, J., and J.-S. Wang, 2006, Phys. Rev. B **74**, 054303.
Wang, J., and J.-S. Wang, 2007, Appl. Phys. Lett. **90**, 241908.
Wang, L., and B. Li, 2007, Phys. Rev. Lett. **99**, 177208.
Wang, L., and B. Li, 2008, Phys. Rev. Lett. **101**, 267203.
Wang, J.-S., J. Wang, and J. T. Lü, 2008, Eur. Phys. J. B **62**, 381.
Wang, J.-S., J. Wang, and N. Zeng, 2006, Phys. Rev. B **74**, 033408.
Wang, J.-S., N. Zeng, J. Wang, and C. K. Gan, 2007, Phys. Rev. E **75**, 061128.
Wang, R.-Q., L. Sheng, R. Shen, B. Wang, and D. Y. Xing, 2010, Phys. Rev. Lett. **105**, 057202.
Ward, D. R., N. J. Halas, and D. Natelson, 2008, Appl. Phys. Lett. **93**, 213108.
Wu, G., and B. Li, 2007, Phys. Rev. B **76**, 085424.
Wu, L.-A., and D. Segal, 2008, Phys. Rev. E **77**, 060101.
Wu, L.-A., and D. Segal, 2009, J. Phys. A **42**, 025302.
Xie, F., K.-Q. Chen, Y. G. Wang, and Y. Zhang, 2008, J. Appl. Phys. **103**, 084501.
Xu, Y., J.-S. Wang, W. Duan, B.-L. Gu, and B. Li, 2008, Phys. Rev. B **78**, 224303.
Yamamoto, T., and K. Watanabe, 2006, Phys. Rev. Lett. **96**, 255503.
Yamamoto, T., S. Watanabe, and K. Watanabe, 2004, Phys. Rev. Lett. **92**, 075502.
Yang, N., G. Zhang, and B. Li, 2008, Nano Lett. **8**, 276.
Yang, N., G. Zhang, and B. Li, 2009, Appl. Phys. Lett. **95**, 033107.
Yang, N., G. Zhang, and B. Li, 2010, Nano Today **5**, 85.
Yang, Z., M. Chshiev, M. Zwolak, Y.-C. Chen, and M. Di Ventra, 2005, Phys. Rev. B **71**, 041402.
Ying, Y., and G. Jin, 2010, Appl. Phys. Lett. **96**, 093104.
Yu, C., L. Shi, Z. Yao, D. Li, and A. Majumdar, 2005, Nano Lett.**5**, 1842.
Yudson, V. I., and V. E. Kravtsov, 2003, Phys. Rev. B **67**, 155310.
Zhang, G., and B. Li, 2005, J. Chem. Phys. **123**, 114714.
Zhang, Z.-Y., 2007, J. Phys. Condens. Matter **19**, 086214.
Zheng, X., W. Zheng, Y. Wei, Z. Zeng, and J. Wang, 2004, J. Chem. Phys. **121**, 8537.
Zhernov, A., and E. Chulkin, 2000, J. Exp. Theor. Phys. **90**, 308.
Zhong, H., and J. R. Lukes, 2006, Phys. Rev. B **74**, 125403.
Zimmermann, J., P. Pavone, and G. Cuniberti, 2008, Phys. Rev. B **78**, 045410.
Zippilli, S., G. Morigi, and A. Bachtold, 2009, Phys. Rev. Lett. **102**, 096804.
Žutić, I., J. Fabian, and S. Das Sarma, 2004, Rev. Mod. Phys. **76**, 323.
Zwolak, M., and M. Di Ventra, 2008, Rev. Mod. Phys. **80**, 141.